SCIENCE & ENGINEERING LIBRARY

SIR GEORGE WILLIAMS UNIVERSITY
LIBRARY

THE TYPOLOGY OF A MANUFACTURED SURFACE AND ITS RELATION TO THE MECHANICAL PROPERTIES.

SEP 20 1971

KUANG-CHUN LIN

A MAJOR TECHNICAL REPORT

IN THE

FACULTY OF ENGINEERING

Presented in partial fulfilment of the requirements for the

Degree of MASTER OF ENGINEERING

at

Sir George Williams University

Montreal, Canada

Date: September 10, 1970

ACKNOWLEDGEMENT

The author expresses his profound gratitude to his dissertation supervisors Dr. T.S. Sankar and Dr. M.O.M. Osman for their valuable guidance and encouragement during all phases of this investigation.

The author also wishes to express his thanks to the Department of Mechanical Engineering for the use of their laboratory facilities. Many thanks are accorded to United Aircraft of Canada Limited for their encouragement and financial assistance.

This investigation forms a part of a research project supported by the research grants A7104 and A5181 from the National Research Council of Canada.

ABSTRACT

The specification and the measurement techniques of the topographical features of a manufactured surface and their relation to the mechanical properties and performance are critically discussed in this dissertation. Existing theories that describe the irregular surface textures are reviewed and compared with a number of data avaible so that useful information on design procedures can be obtained. The latest techniques employing probabilistic descriptions are also included.

To verify the effect of cut-off on the Center Line Average (CLA) measures and its relation to the wave length of the secondary texture, an experiment was conducted with Talysurf No. 4 instrument. Five different surface samples were measured and the roughness profiles were obtained. It is observed that the CLA value increases with an increase in cut-off.

The complex problem of correlating the topographical description of a surface profile to mechanical behaviors such as fatigue strength, bearing capacity, ability to retain lubrication, wear, and corrosion are all respectively discussed and general conclusions are drawn. It is concluded that both the surface roughness and the surface hardness affect the fatigue strength. Compressive residual stresses are found to increase the fatigue strength whereas tensile residual stresses lower the resistance of the component against fatigue. It is noted that, in general, the load carrying capacity can be increased with a smoother finish for a shaft. Further, use of high viscosity lubricant yields a higher bearing load capacity for a smooth surface than for a rough surface. The results derived are useful for specifying the desired quality of finish for a surface in relation to the functional usefulness of the component that has been designed to provide a specific performance.

RÉSUMÉ

La spécification et les techniques de la mesure des traits topographiques d'une surface usinée, leur rapport aux propriétés mécaniques et la performance sont discutés sérieusement dans cette dissertation. Les théories existantes qui décrivent les textures irrégulières de la surface sont revues et certaines vérifications expérimentales sont faites pour fournir d'utiles informations sur les procédes d'un dessin. Les plus récentes techniques qui emploient des descriptions probables sont aussi incluses.

Afin de vérifier l'effet d'une coupure sur les mesures de la courbe centrale médiane (CCM) et sa relation avec la longueur d'onde de la texture secondaire, une expérience fut élaborée à l'aide de l'instrument No. 4 Talysurf. Cinq différents échantillons de surface ont ete mesurés et les profils de rudesse ont été obtenus. On peut observé que la valeur de la courbe centrale médiane augmente avec l'augmentation de la coupure.

Le problème complexe d'associer la description d'un profil d'une surface aux comportements mécaniques tel que l'endurance, la capacité de soutenir, l'abilité de retenir la lubrification, l'usure et la corrosion sont tous respectivement discutés et des conclusions générales en sont tirées. Comme conclusion on peut voir que la surface rude et la surface dure affecte l'endurance à la fatigue. On découvre que les forces compressives résiduelles augmentent l'endurance mais que les forces de tension résiduelles baissent la resistance de la pièce contre l'endurance. On peut noter qu'en général la capacité de supporter une charge peut être augmentée avec un fini plus lisse pour le cas d'un

arbre. En plus, l'usage d'un lubrifiant à haute viscosité produit une capacité de charge de roulement plus élevée pour une surface lisse plutôt que pour une surface rude. Les résultats dérives sont utiles pour spécifier la qualité du fini désiré pour une surface en rapport avec l'utilité fonctionelle de la pièce qui a été conçue pour fournir une performance spécifique.

TABLE OF CONTENTS

CHAPTER 1

INTRODUCTION

The topic of typology of manufactured surface is primarily concerned with the specification and measurement of the topographical features of surfaces. Any surface typological feature comprising of minute hills and valleys, that occur at regular or irregular intervals, tends to form a kind of pattern or texture and is usually called surface roughness.

Till recently the most widely accepted standard for the measurement of surface roughness is the so called Centre Line Average (CLA) value which gives a measure based on the average of the height of the hills and depth of the valleys with respect to the centre line. Electronic instruments are employed for the measurement of the CLA value. For surfaces that are obtained through machining, the roughness is always inseparable from whatever finishing process that is employed. For example, abrading processes, such as lapping and honing, produce a texture irregular and multi-directional; grinding, which is the most widely used finishing process, generally gives a texture which is irregular but unidirectional; while the textures produced by the cutting processes, such as turning, boring and shaping etc., tend to be both evenly spaced and uni-directional. It may be seen that each machining process has a typical effect on the nature of surface produced which along with the actual texture influences the physical and mechanical properties of the resulting product. Hence when a specification is made for the required roughness, it is automatically necessary to specify the finishing process also.

Even for a particular scheme of machining operation, the surfaces

produced can be extensively influenced by the mode of metal removal action. The influencing factors generally are (see ref. 16):

(i) plastic deformation as a result of cold work,

(ii) phase transformation and recrystallization,

(iii) intergrannular attack and preferential solution of micro-constituents,

(iv) microcracking and macrocracking,

(v) change in hardness of surface layer,

(vi) residual stress distribution in the surface layer,

(vii) embrittlement by chemical adsorption of elements such as hydrogen or halogens,

(viii) spattered coating of remelted metal deposited on the surface during electrical discharge, electron beam or laser machining.

This listing only shows that the mechanism of metal removal also plays an important role in the finishing of surfaces besides the actual machining process employed. The extent of each of these effects is different for different process, and further the stress conditions, hardness, and structure of the subsurface layer also play an important role in determining the properties of the surface. All the factors mentioned above affect the principal physical and mechanical properties such as fatigue strength, bearing capacity, coefficient of friction and lubricability which define the quality of the manufactured surface in relation to its performance.

Extensive efforts (3, 24) have been made in the past years to search for a finite number of parameters which can relate the roughness directly or indirectly to the physical and mechanical properties of the manufactured surfaces. All the theoretical and experimental evaluations showed just the dependence of each of the aforesaid physical properties on the individual

surface characteristic and the search for the parameters to describe this interdependency still continues.

The dissertation presented here is mainly concerned with a detailed discussion of the relationship of the surface topography to the physical properties associated with it. A critical assessment of all the important theories and experimental findings is made and conclusions are drawn for purposes of determining design criteria. Proposals are made where improvements on the existing techniques are desired.

Mention must be made here to stress the influence of the quality of a finished surface on the functional usefulness of the component in the specific mission for which the design has been carried out. As far as the properties and performance of the product are concerned, the degree of roughness of the surface will affect its function as an integral part of the system. Among these some of the important factors are (see ref. 13):

(i) the friction and wear between unlubricated surfaces are increased with an increase in their roughness,

(ii) the danger of seizure in lubricated surfaces is reduced for smooth surfaces,

(iii) interference fits made on rough surfaces may have a reduced area of contact and a consequent reduction in the holding ability of the joint,

(iv) fluid flow in small passages such as orifices and valves is reduced if the roughness of the wall is increased,

(v) fatigue strength of parts is increased as the surfaces become less rough.

(vi) bearing capacity is increased for smoother surfaces in contact.

As mentioned before, theories and experiments available to equate surface texture to its physical properties are numerous. Yet, none of

the investigations have produced universally acceptable results that design engineers could adopt. For example, even a rigorous description (see ref. 24) of a surface profile is lacking for specification purposes. An attempt is made here to establish some useful theoretical and experimental relations on surface roughness and its mechanical qualities based on existing literature.

Chapter 2 of this report reviews the different surface descriptions and measuring techniques proposed in existing works. Some sample surface profiles are shown to elucidate their variety from actual measurements made in the laboratory. Analytical studies based on probabilistic characteristics of a surface texture are discussed in detail in Chapter 3. Such statistical descriptions are based on mathematical theories of stochastic processes and hence are more reliable than other types of analytical investigations. In Chapter 4 the correlation between the surface roughness and the fatigue strength of manufactured parts are dealt with and the effect of residual stresses due to different manufacturing processes are also reviewed. Using the results available from existing works on this subject, certain design criteria are also presented. Some experimental results of previous investigators on the lubrication characteristics of components having different surface roughnesses are discussed in Chapter 5. An analytical approach using stochstic processes to evaluate the relation between the load and the frictional forces for lubricated slider mechanism is also included in this Chapter.

Chapter 6 is devoted to the effect of surface roughness on bearing area, bearing capacity and coefficient of friction. A brief discussion on resistance to corrosion of materials having different surface roughnesses is presented in Chapter 7. General conclusions based on the material

presented in all these chapters are drawn in Chapter 8.

An extensive list of important literature on the subject matter of this dissertation is provided at the end. References to this bibliography in the body of this dissertation are indicated by means of parantheses. The notations used are explained as and when they appear in the text.

CHAPTER 2

SURFACE ROUGHNESS AND EXISTING MEASURING TECHNIQUES

2.1 Introduction:

Specification of finish for a surface is of increasing importance to design engineers. As noted in the introductory chapter, the roughness of a surface can influence fatigue strength, bearing capacity, retaining of lubrication, rate of wear, corrosion resistance etc. of a manufactured product.

2.2 Kinds of surface irregularities (1):

The surface irregularities produced by different machining processes may be classified into four kinds:

(i) irregularities within each tool mark or abrasive scratch mark resulting from the way in which the metal has been torn or otherwise detached from the work piece,

(ii) the tool or scratch marks from whose appearances it may be possible to deduce the type of the machining processes involved,

(iii) the irregularities arising from defects in the process itself such as chatter marks, imperfect truing of a grinding wheel or setting of a milling cutter,

(iv) general form errors due to the imperfection in the machine, for example imperfect slideways etc.

The first two kinds of irregularities, which are the natural and inevitable consequences of the process as carried out in a substantially perfect machine, are defined as "roughness". The third kind of irregularity which, theoretically, should not occur is defined as "waviness". The fourth

kind of irregularity is generally deemed to lie outside the field of surface texture. When both waviness and roughness are present, they must be separated as far as possible if a measurement on roughness is needed. The general case showing a secondary surface texture which includes the form error is illustrated in Fig. 2.1. A short length L_1 will serve to isolate the primary texture and give a value (peak-to-valley, for simplicity) for H_1. If the length is increased to L_2 the waviness will also be included and the value will rise to H_2. When the whole length L_3 of the surface is adopted the total height measured will be H_3.

2.3 Instrumentation characteristics:

Instruments which measure surface roughness are designed to examine comparatively short lengths of surfaces so that the effect of waviness is minimized. Cut-off lengths as recommended vary from 25 m.m.(1 in.) to .08 m.m. (.003 in.), although a typical range for a given instrument might be .25 m.m. (.01 in.), .8 m.m. (.03 in.) and 2.5 m.m. (.1 in.). The length chosen should be long enough to accomodate the surface generation characteristics of the metal shaping process; for instance, if a turned surface is being examined it may not exceed the feed per revolution (see 2).

2.4 Existing measuring techniques (3, 4):

Among the many aspects of the irregularities to be measured, the height of peaks and the depth of valleys seem to be most useful. As it is not generally desirable to rate the surface only on the basis of the highest peak and the deepest valley, some method of averaging become necessary.

All methods so far proposed require first a determination of a

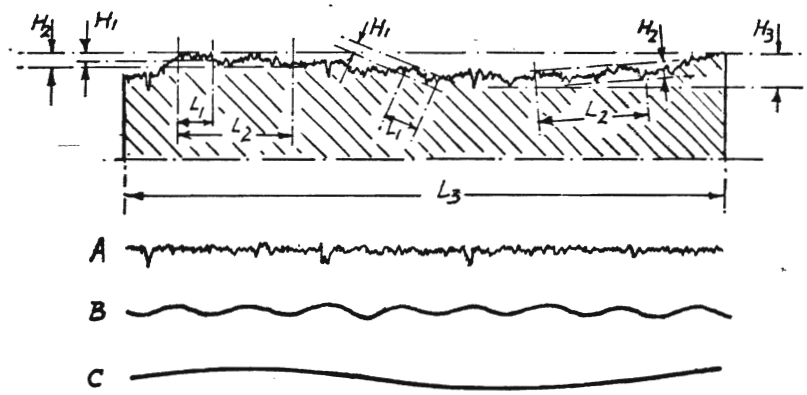

Fig. 2.1 General case of scratch texture due to tool abrasion.

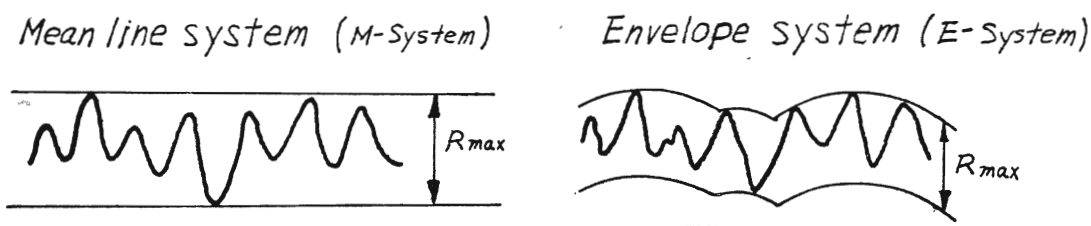

R_{max} = Rautiefe ≡ Peak to valley height

Fig. 2.2 Peak to valley measure.

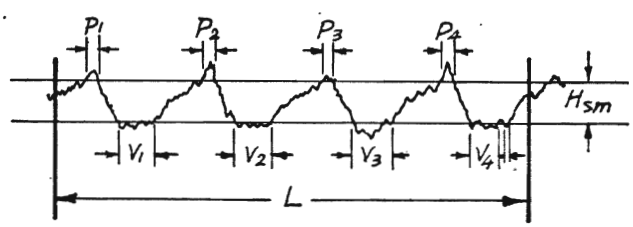

$$\Sigma P = \frac{L}{20} \qquad \Sigma V = \frac{V}{10}$$

Figure 2.3 The Swedish method.

reference line with respect to which the peaks and valleys are to be measured. In most systems, the shape of the reference line is defined independently of the irregularities and is generally given by the shape shown on the design drawing, (M-system). In a recent proposal by von Weingraber (14) the shape of the reference line is determined by the irregularities themselves and is not open to independent definition, (E-system).

Some of the important types of surface measures are:

(i) Peak to valley measure and is illustrated in Fig. 2.2. Some of the countries using standards based on such concept are Germany DIN 4762, Swiss VSM 58300, U.K. B.S. 1134, International ISO Rec 468. For both M-system and E-system the measured value is

R max. = R autiefe = peak to valley height.

(ii) Swedish method which is based on peak and valley intercepts, is shown in Fig. 2.3. In the diagram P stands for peak intercept while V stands for valley intercept, and L is the measured length of surface. When $P = \frac{L}{20}$, $V = \frac{L}{10}$, then the measured value is the distance H_{sm} between the two intercepting lines, where H_{sm} is the height as referred to the Swedish method.

(iii) British method where the mean difference is taken between the five highest peaks and the five lowest valleys. This is called the ten point height and is given by the formula

$$\frac{(h_1 + h_2 + h_3 + h_4 + h_5) - (h_6 + h_7 + h_8 + h_9 + h_{10})}{5} \quad \ldots(2.1)$$

where h_1 to h_5 are heights of the highest peaks & h_6 to h_{10} are heights of the lowest valleys measured from a specified datum within a length of surface measured.

(iv) Mean line measures, standards based on this are U.K. B.S. 1134, U.S.A. B46.1, International 468. The mean line has the nominal shape of a defined length of the surface, and is so positioned such that the sum of the squares of equally spaced ordinates measured from it has a minimum value. The mean line can be easily located using electronic integrating instruments. This is also called "centre line average", and is described in Fig. 2.4. The formula for the measured values are

$$\text{CLA} = \frac{1}{L} \int_0^L |y| \, dL , \quad \ldots\ldots\ldots\ldots\ldots (2.2)$$

$$\text{rms} = \left(\frac{1}{L} \int_0^L y^2 dL.\right)^{\frac{1}{2}} \quad \ldots\ldots\ldots\ldots\ldots (2.3)$$

CLA or AA (arithmetic average) is much easier to measure and is used widely in specifications. The values of CLA measured over a given surface area exhibit very little scatter when compared with peak to valley height R max. The rms value is usually 10 to 30% larger than the CLA value.

(v) Crest line measure:

The principle of this surface measuring technique is illustrated in Fig. 2.5. The formulas are

$$G_M = \frac{1}{L} \int_0^L y \, dL , \quad \ldots\ldots\ldots\ldots\ldots (2.4)$$

$$G_E = \frac{1}{L} \int_0^L y \, dL . \quad \ldots\ldots\ldots\ldots\ldots (2.5)$$

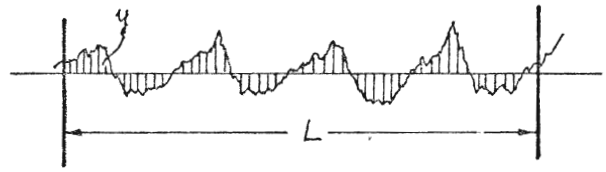

$$CLA = \frac{1}{L}\int_0^L |y|\,dL \qquad RMS = \sqrt{\frac{1}{L}\int_0^L y^2\,dL}$$

Fig. 2.4 Mean line measure (CLA).

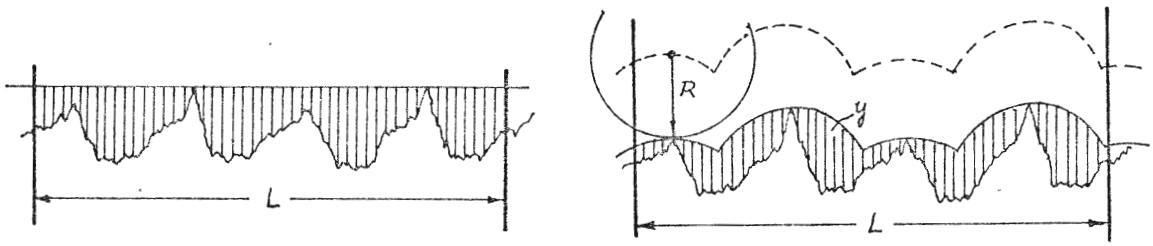

$$G_m = \frac{1}{L}\int_0^L y\,dL \qquad G_e = \frac{1}{L}\int_0^L y\,dL$$

Fig. 2.5 Crest line measures.

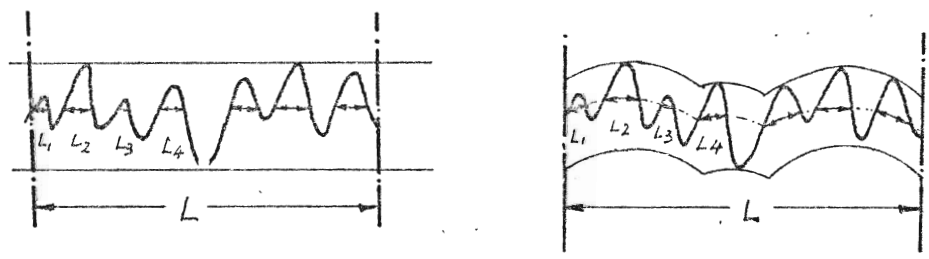

$$t_p = \frac{\Sigma L_i}{L} \times 100 = Traganteil \equiv Bearing\ ratio$$

Fig. 2.6 Bearing ratio curve.

G value means Glättungstiefe, or levelling depth, the subscript M stands for the M-system and the subscript E for the E-system. They are aimed at the separation of roughness, waviness and errors of form by a proper choice of the rolling circle radius. Because the mean line measure also offers the same separation characteristics through a proper choice of the sample length and uses a simple measuring instrument, the crest line measure has not been widely used in practice.

(vi) Bearing ratio curve: This is based on the bearing area after a certain amount of wear as shown in Fig. 2.6. The measured value at a certain amount of wear is given by the formula

$$t_p = \frac{\Sigma L_i}{L} \times 100\%, \quad \ldots\ldots\ldots\ldots\ldots (2.6)$$

where L_i = length of intercept at ith peak,

L = length of surface measured.

2.5 Critical comparison of the measuring methods (4, 5, 6):

All methods explained so far measure just aome value of the irregularity height and are purely arbitrary in the sense that they bear no direct physical relation to the total description of a surface. They only serve to compare the surfaces produced by the similar manufacturing processes. Further, no indication is given about the shape of the surface profile and it is possible that profiles which are completely different in shape may have the same average height.

The Swedish method possesses a merit of indicating directly the dimensional change that would result from lapping off the bulk of the scratch marks. The British "ten-point height" can aid to make a quick assessment of interference fringes seen through a microscope. But neither

of the two methods lends itself for incorporation in direct reading instrumentations.

The principles of centre line methods lend themselves to simple direct reading instrumentation. The CLA value is best regarded simply as an index by which a defined manufacturing process can be rated and controlled. The G values in M and E-systems can generally be determined from a profile graph more readily than the CLA method but instruments based on this measuring system are only in the experimental stages and desirable radius of the rolling circle has not yet been exactly determined.

Laboratory techniques are now available for recording the surface data on punched tape and inputing via a converter into a digital computer. With these advancements statistical research into such parameters as average slope, high spot counting and bearing area (Tragenteil) are reported in the literature (see 12).

Of all these measures described in previous pages, no two are exactly convertible, though some are reasonably convertible at least for a given machining process. For instance, for a particular surface the relationship between rms and CLA values is as follows:

Machining process	rms / CLA
Turning	1.1 to 1.15
Grinding	1.15 to 1.2
Lapping	1.3

According to von Weingraber (14), the ratio of G value to CLA value varies from 1.85 for lapping to 3.0 for shaping; for ordinary range of grinding, this ratio extends only from 1.8 to 2.6. By an independent test performed at Taylor-Hobson Laboratory the mean ratio of G value to

CLA value for grinding was confirmed to be 2.4. Investigation by Diachenk (5) showed, for a variety of frequently encountered surfaces, that the ratio of the height based on Swedish method to the CLA value is around 4, while that of the ten-point height to CLA is around 5.

2.6 Laboratory devices for topographic assessment of surface texture:

Plan view of the texture may be observed through the use of a laboratory microscope. But the conditions of illumination can greatly affect the appearance of the image, so also any small changes in focus. It can be very selective in what it reveals because it tends to create an illusive deduction whenever peaks and valleys of large inclinations are observed (see 7).

Oblique cross-sections and topographic contours can be obtained by the interference method. In principle, the method employs an optical flat plate. When the instrument is put on top of the specimen and a beam of collimated monochromatic light is projected on it, the light rays will be reflected partly by the flat under-surface of the optical test plate and partly by the surface of the specimen. By setting a certain inclination for the optical test plate, the beam reflected from the specimen will have a phase lag in time, as compared to the beam reflected from the test plate. The resulting interference fringes will trace the oblique sections of the texture (7). If the inclination of the optical test plate is zero with the specimen a simple contour map of the surface can be obtained.

Cross-sections normal to the surface using stylus instruments is another measuring technique. The stylus is generally a pyramidal or conical diamond with a flat or round tip. U.S. standard calls for a 60° cone with a radius of .0005 in. at the tip. In U.K. a 90°

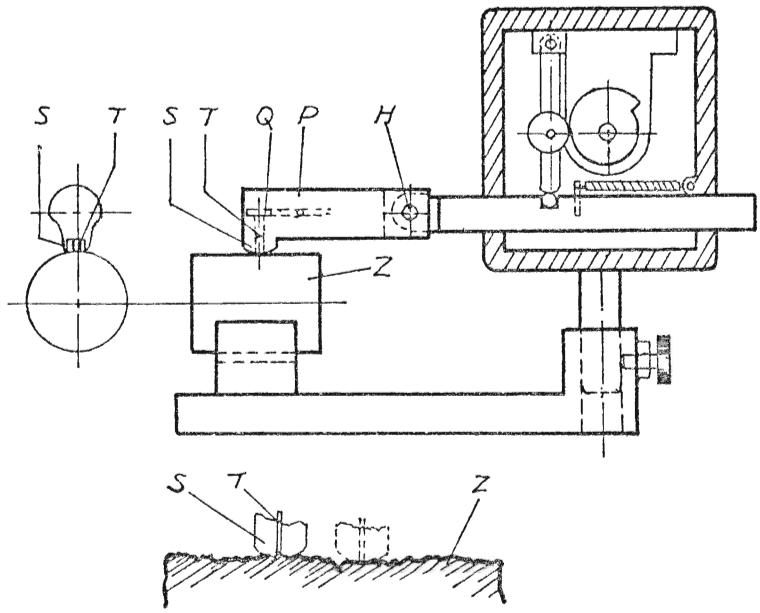

Fig. 2.7 Principal parts of stylus device.

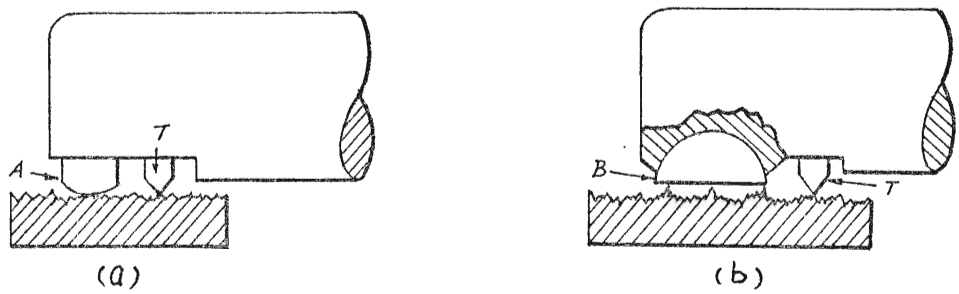

Fig. 2.8 Rounded skid and swiveling shoe adopted in stylus devices.

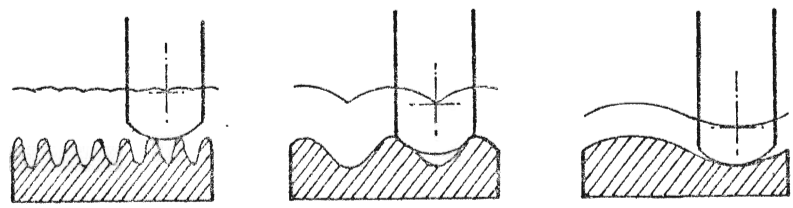

Fig. 2.9 Effect of wave form on skid movement.

pyramidal form, with a flat or rounded tip not more than .0001 in. in width or radius is generally employed. A useful guide to the maximum permissible load on the stylus is given by a formula in the American Standard B-46/1955, which states

Maximum force in grammes

$$= .00001 \times (\text{Tip radius in micro-inches})^2$$

A stylus instrument in which the datum is generated by a rounded skid S sliding across the surface is shown in Fig. 2.7. This is an approximate measuring device that is widely used. The pick-up body P is hinged to the driving mechanism at H, and provided with a pair of rounded feet S adjacent to the stylus T, at least one of the feet resting on the specimen Z and sliding across it together with the stylus. Q represents a displacement sensitive device. Fig. 2.8 shows two general types of feet used for the stylus devices. A is generally called a rounded skid, and B is known as a swivelling shoe. T represents the stylus. The instrument directly gives the vertical movement of the stylus relative to the skid or shoe.

When the skids are used, the datum generated is the locus of the centre of curvature of the skid as it slides over the surface. When the principal crests are close enough together, the locus may approximate closely to its true form as shown in Fig. 2.9. When the spacing increases so will the movement of the skid, until finally it moves up and down as much as the stylus. When the spacing is irregular, some undulations may be exaggerated and some other undulations diminished in such a way that even though the graph is not in a sense accurate it still gives approximately the right impression of the surface. The practical limits of the skid sre therefore not calculable and have to be gained from experience.

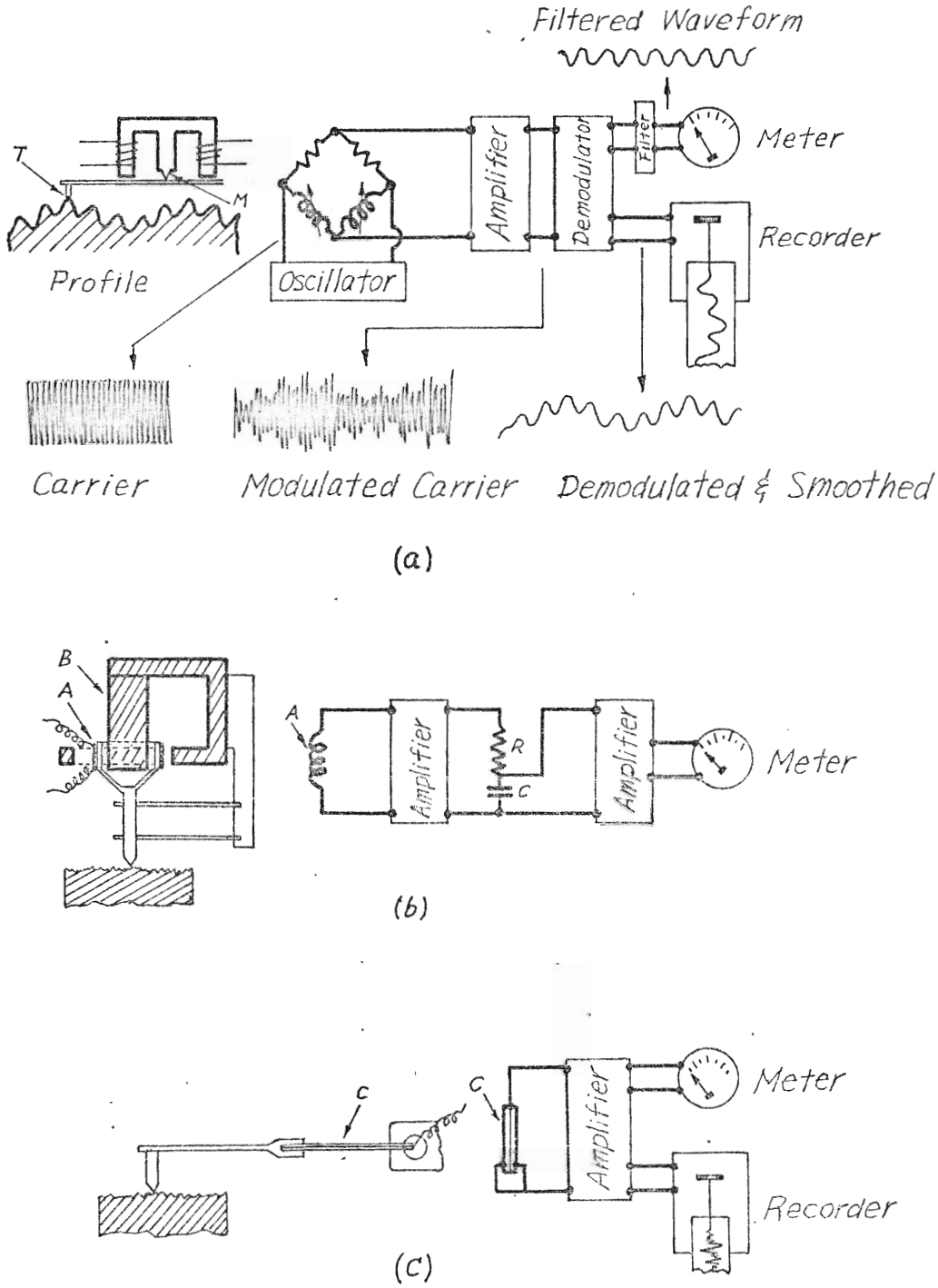

Fig. 2.10 Electrical Magnifying Device with Circuits.

(a) for carrier modulating instrument,

(b) for current generating instrument,

(c) for potential generating instrument.

The difficulties resulting from the adoption of a skid can be largely avoided by means of the shoe shown in Fig. 2.8 (b). Provided the crests are reasonably uniform in level and are spaced apart by not more than half the length of the shoe, a very serviceable datum can be obtained.

Generally, skids are satisfactory for finer cut and abraded surfaces, for which the characteristic spacing is less than .03 in. The properties of skids and shoes are discussed by Reason and Hopkins (1).

Magnifying devices are sometimes used in making surface profile observations. Among all the magnifying devices those based on electrical methods are most practical. They can produce not only a graphical profile but also a numerical assessment of the surface. They can be classified mainly into two basic categories:

(i) Carrier modulating devices, in which the magnitude of a current (the carrier) is controlled (modulated) at every instant according to the position of the stylus relative to the datum, regardless of how long the stylus remains in a given position.

(ii) Current or potential generating devices, in which a current or potential is generated according to the motion of the stylus as it is displaced from one level to another.

Fig. 2.10 describes the electrical principle behind, (a) the carrier modulating instrument, (b) the current generating instrument, and (c) the potential generating instrument. Fig. 2.10 (a) shows the circuit diagram used in the Talysurf Model 3 instrument, where a number of E-shaped stampings with coils are mounted inside the pick-up. An armature

M carrying a stylus T is pivoted over the central limb so as to leave small air gaps between the armature and each limb. The two outer limbs form two differential air gapped inductances whose impedances depend on the width of the air gap. A high frequency AC flows through each of the coils, the magnitude of the current being proportional to the impedance of the coils. Thus the position of the stylus modulates the carrier. According to this circuit, the current passing to the amplifier is proportional to the changes in air gaps. The amplified signal is demodulated to show the motion of the stylus. The output signal can be further amplified and used for controlling a recorder or actuating an integrating meter. Before entering the integrating meter, it is generally filtered to suppress the low frequencies and confine the measurement to the higher frequencies of the texture.

In Fig. 2.10 (b) the stylus is attached to a coil which is located in a permanent magnetic field. As the stylus moves up and down current is generated in the coil, and the amount of current is proportional to the amplitude of the stylus motion. After amplification and filteration by a R-C circuit, the meter readings are obtained. In Fig. 2.10 (c), the motion of the stylus generates an e.m.f. in proportion to the amplitude, which after amplification is used to actuate the meter or the recorder. In the last two instruments the current or potential produced is also dependent on the velocity of the stylus travelling over the surface measured, therefore they are not widely used.

Suppose several surfaces of different irregularities as formed by equally spaced sine waves with different wave lengths λ as shown on the top of Figure. 2.11 are considered. For a very small value of λ, the stylus may not be able to enter all the grooves, and hence there will be

practically very few readings observed in the carrier modulating type of instrument. As the value for λ increases, the response of the instrument will increase. But once the stylus is able to enter the bottom of all grooves freely, there will be no further increase in the readings, however large the wavelength becomes. This characteristic is shown by the solid line in Fig. 2.11 and is known as transmission curve. Since the output of the instrument is dependent on the actual motion of the stylus, it may be expected to fall off below a certain frequency level, that is, above a certain λ as indicated by the dotted line in Fig. 2.11. Only within the range x-y of the flat solid line the output plot is useful as a measure of the surface amplitude. The range between x and y is called the "pass band". This type of characteristic is required inherently for instruments based on average measures, so that the entire sampling length can be covered in regular steps and CLA values obtained. This is achieved in carrier modulating instruments, by a wave filter in the path of the current actuating the averaging meter. The rate of attenuation accepted in U.K. & U.S.A. can be provided by two R-C networks of equal time constant connected in cascade as shown in Fig. 2.12. The time constant (in seconds) for the network is given by Resistance (in Ohms) multiplied by Capacitance (in Farads). That is,

$$\frac{e}{E} = \frac{R}{\sqrt{R^2 + \left(\frac{1}{2\pi fc}\right)^2}} \qquad \ldots\ldots\ldots\ldots\ldots\ldots (2.7)$$

and the accompanying phase shift is equal to $\frac{1}{2\pi fcR}$. When two circuits of equal time constant are used, the final output is given by

$$e_{out} = \left(\frac{e}{E}\right)^2. \qquad \ldots\ldots\ldots\ldots\ldots\ldots (2.8)$$

The combination of attenuation and phase shift may cause some distortion of wave-forms having significant frequencies coming just around the

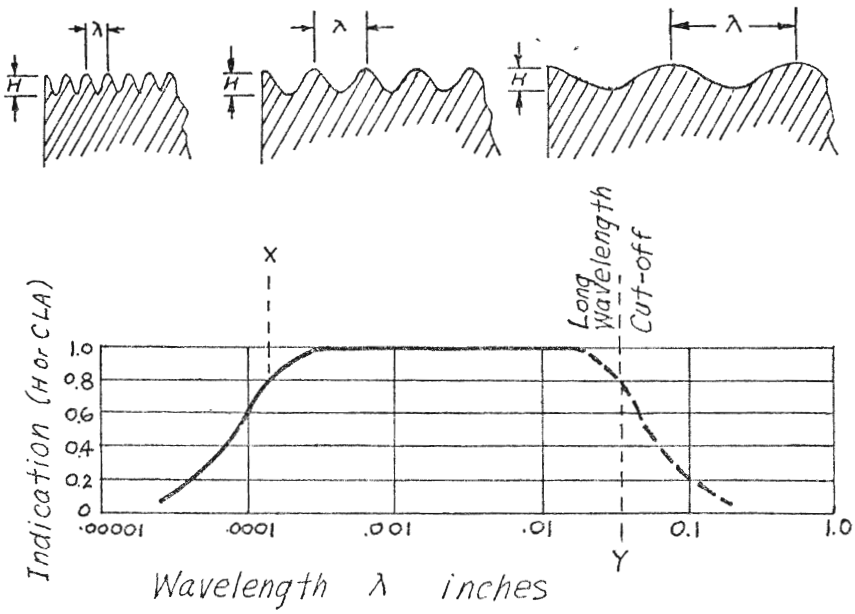

Fig. 2.11 Operative effect (transmission characteristic) of electric wave-filter.

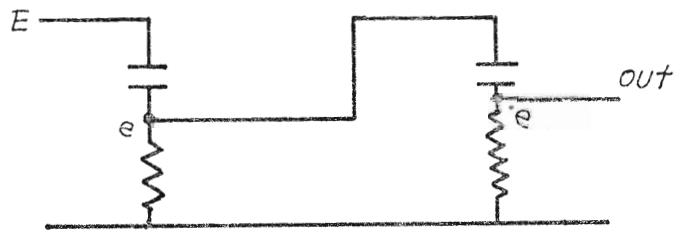

Fig. 2.12 Line diagram of R-C networks of wave-filter.

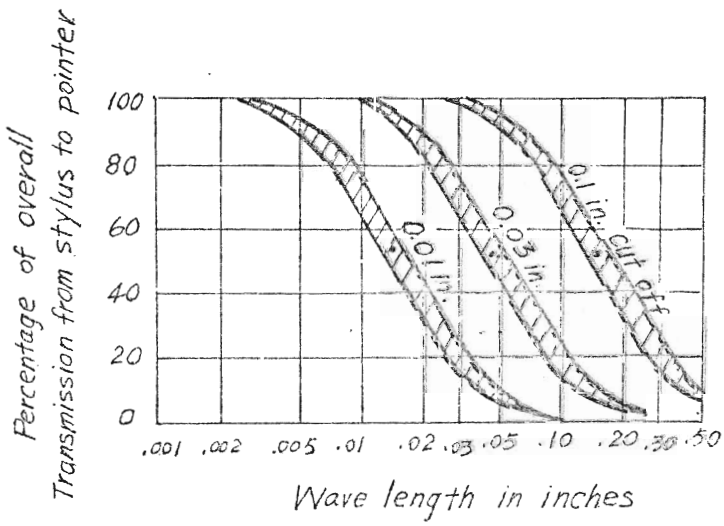

Fig. 2.13 Transmission curves of standard R-C wave-filter.

cut-off. But its effect on the averaged reading is very little (1). As an illustration, Fig. 2.13 shows standard 2 R-C wave-filter transmission curves with cut-off .01, .03 & .10 inches at 75% transmission from stylus to meter pointer.

Because of its simplicity in assessment and instrumentation, the CLA measure is so far the most widely accepted standard for surface roughness, and therefore the stylus devices with rounded skids and carrier modulating magnification are very popular in application. In order to minimize the effect of waviness, filters having 3 cut-off lengths are inherently attached to the electrical measuring unit. Up to now, Canada, U.K., U.S.A. are the major countries that adopted this system of surface roughness.

2.7 Experimental set-up:

A Talysurf # 4 instrumental set-up was used to measure different samples of manufactured surfaces. The block diagram for the Talysurf device is illustrated in Fig. 2.14.

A gearbox drives a pick-up across the surface at low speeds and a sharply-pointed stylus traces the profile of the surface irregularities. The pick-up is an indicative type transducer, connected in a bridge circuit, in which the vertical movements of the stylus modulate a carrier waveform. The output signal is amplified, demodulated and used for operating a recorder. The signal, suitably modified by employing some filters, is also used to operate the meter that measures the CLA values.

2.8 Results of Experiment:

Five different surface samples were measured. The specifications and test results are given in Table 2.1:

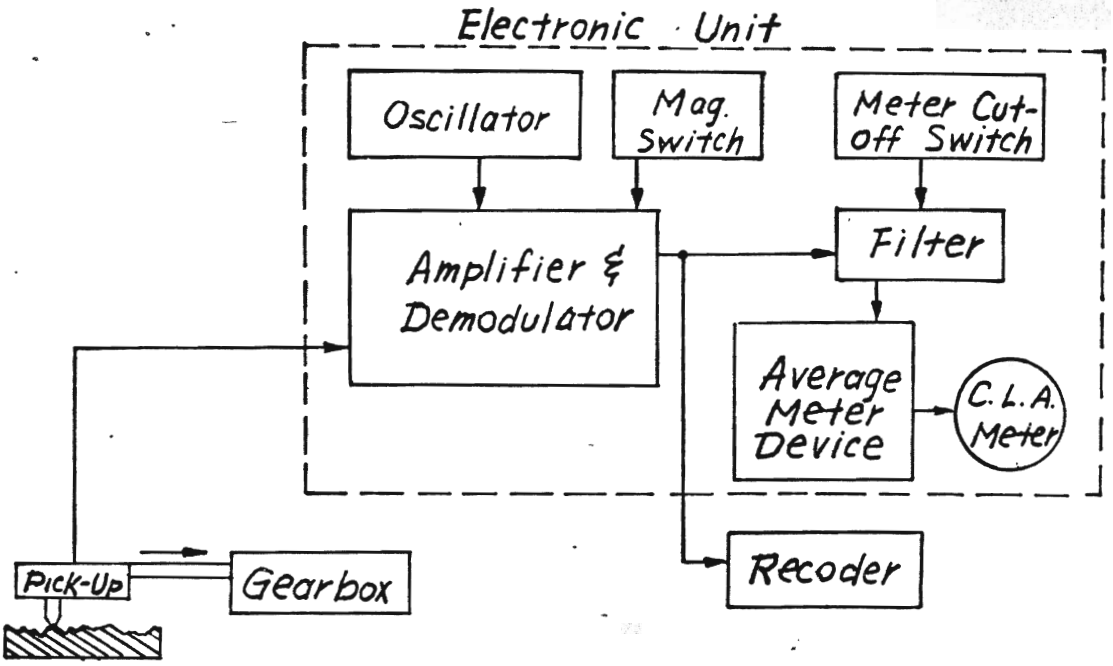

Fig. 2.14 Block diagram of Talysurf No. 4 instrument.

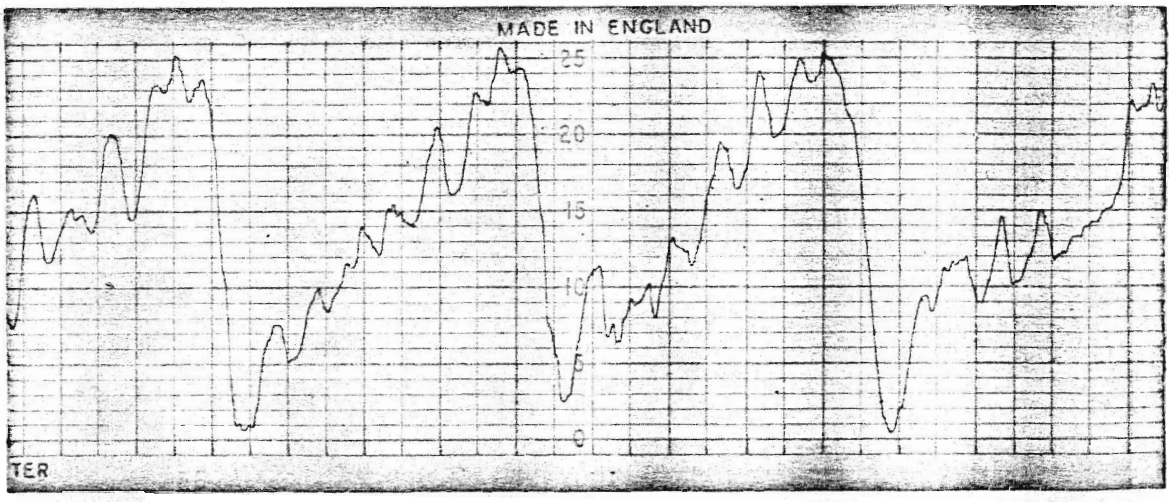

Fig. 2.15(a) Roughness profile in medium turning, X2000V, X100H, CLA = 5.3μm. 0.1 in. cut-off.

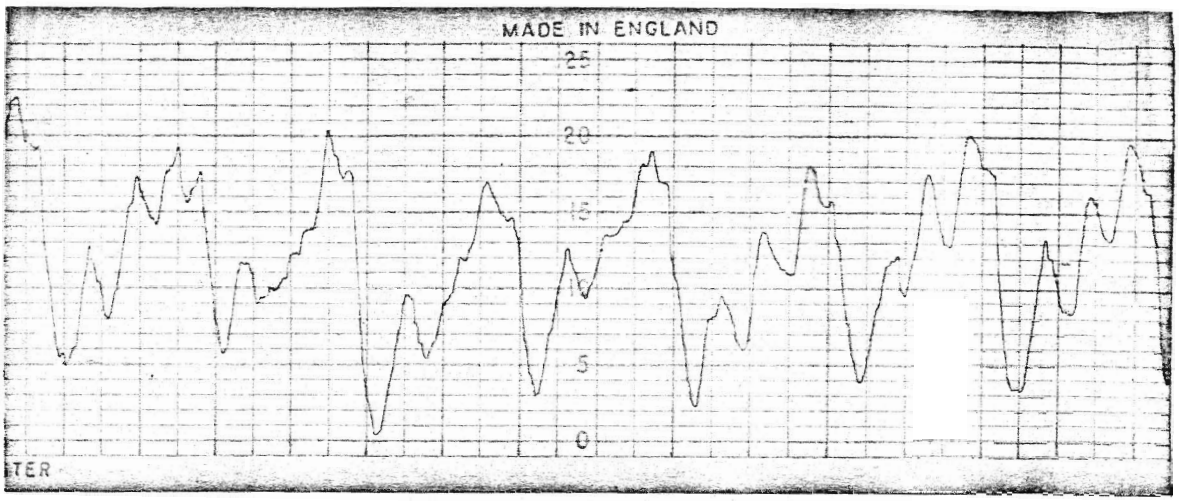

Fig. 2.15(b) Roughness in semi-finish turning, X2000V, X100H, CLA = 3.5μm. 0.1 in. cut-off.

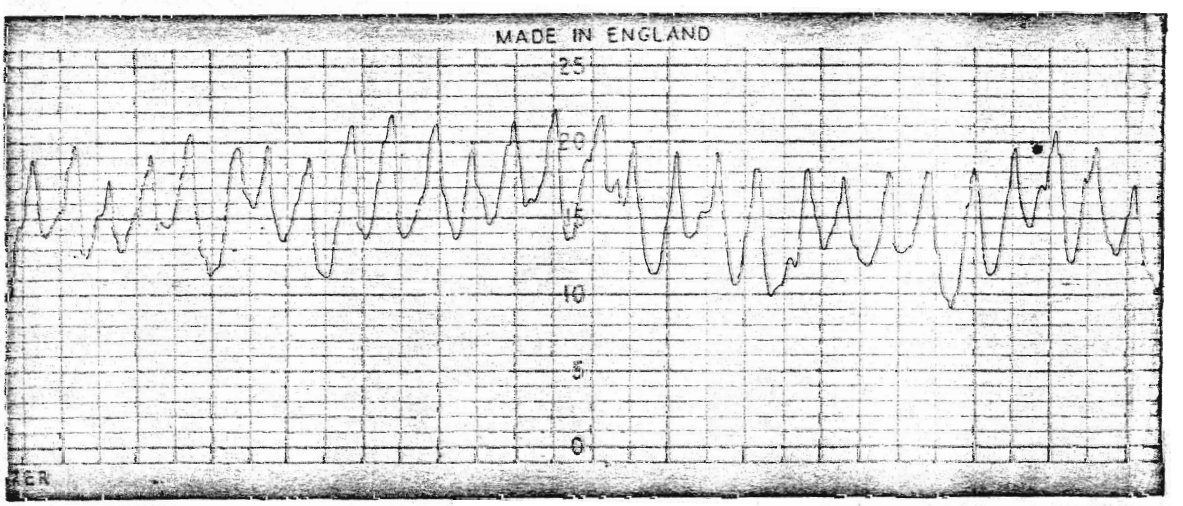

Fig. 2.15(c) Roughness profile in finish turning, X2000V, X100H, CLA = 2.5μm. 0.1 in. cut-off.

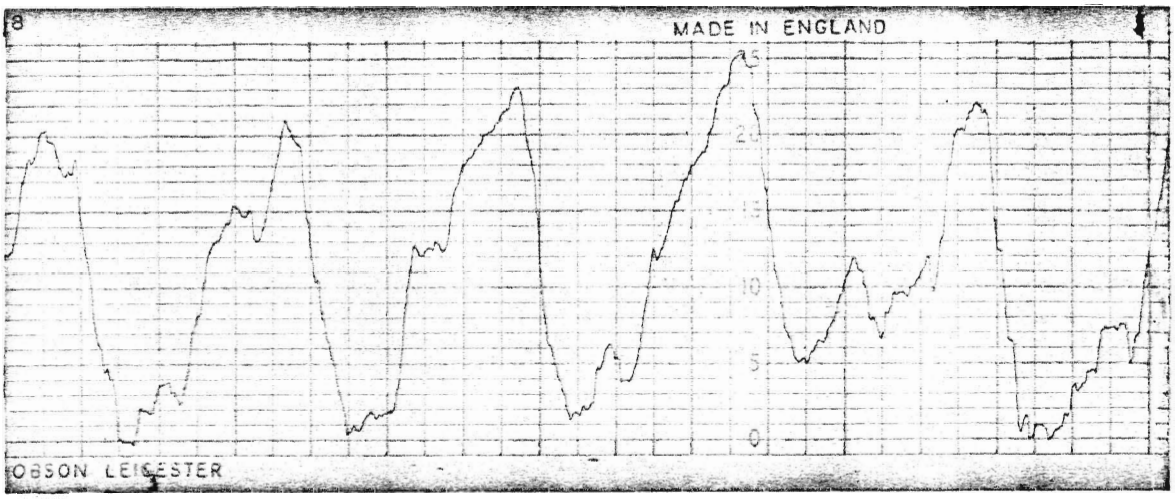

Fig. 2.15(d) Roughness profile in milling, X2000V, X100H, CLA = 5.7μm. 0.1 in. cut-off.

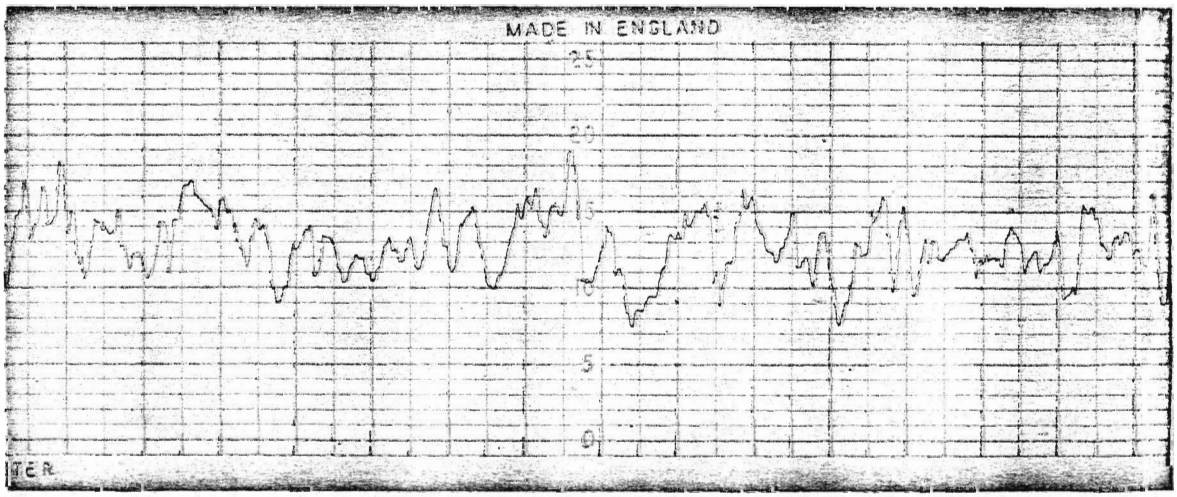

Fig. 2.15(e) Roughness profile in grinding, X2000V, X100H, CLA = 1.7μm. 0.1 in. cut-off.

Table 2.1 Specimen specifications & test results.

Specimen No.	Machining process	Material	RPM	Feed in./Rev.	CAL reading
1	Medium turning	C12 L14	639	.017	5.3 μm.
2	Semi-finish turning	C12 L14	639	.008	3.5 μm.
3	Finish turning	C12 L14	639	.002	2.7 μm.
4	Milling	SAE 1020	317	3.56in./min.	5.7 μm.
5	Grinding	SAE 1020	2750	——	1.7 μm.

By using the recording unit, the roughness profile graphs were plotted for a vertical magnification of 2000 and a horizontal magnification of 100 as shown in Fig. 2.15.

To verify the effects of cut-off on the CLA readings, two tests were made on specimens No. 1 & 2, the results are shown in Table 2.2. If the feed is considered as the wave length, these results are consistent with the transmission curves shown in Fig. 2.13.

Table 2.2 Effect of cut-off on transmission.

Specimen No.	Cut-off	.10 in.	.03 in.	.01 in.
1	CLA value	5.3 μm.	5.1 μm.	3 μm.
	Percent of transmission	100%	96%	56.6%
2	CLA value	3.5 μm.	3.4 μm.	2.8 μm.
	Percent of transmission	100%	97%	80%

2.9 Summary:

After an investigation of the above results, the following remarks are worthwhile mentioning.

(i) The resulting CLA values for each specimen are repeating, the differences are around 1 to 2%. This means the roughness of the specimen surfaces is uniform.

(ii) The effect due to the change of cut-off on the transmission percentage is consistent with the transmission curves shown in Fig. 2.13.

(iii) By measuring the mean distance between every two peaks of the profiles shown in Fig. 2.15 (a), (b) & (c), one gets .0175, .0081 and .0022 inch. respectively, whereas the actual feeds for turning these specimens are .017, .008 and .002 inch. This can provide a check for the profile graphs.

(iv) Since all the profile graphs have the same multiplication factors in both horizontal & vertical directions, their relative roughnesses can be compared by inspecting the graphs.

(v) From Fig. 2.15 (a) it may be found that its peaks & valleys almost have equal area, whereas in Fig. 2.15 (d) one will find that the area of valleys is larger than that of peaks. Even-though the maximum depth of the valley in (a) and (d) are about equal. Thus one can say that sample (d) has larger CLA value.

(vi) By similar reasoning, the bearing area ratio t_p of (a) is higher than that of (d) at the same depth from the tip.

CHAPTER 3

STATISTICAL DESCRIPTION OF SURFACE PROFILE

3.1 Introduction:

To meet design specifications, the use of a single roughness value such as CLA, rms or G_E etc. mentioned in Chapter 2 to describe the surface characteristics is not sufficient. Even though surfaces manufactured by different machining processes may have the same roughness value, they can have different "type" of texture, and hence can exhibit completly different properties as far as fatigue, bearing capacity, frictional resistance, lubricability etc. are concerned. This poses an extremely difficult question. To what degree can further information be obtained by additional measurement values or by a reasonable interpretation of the graph or by establishing a certain suitable typology for the shapes of the irregularities ? It was noted in Section 2 of Chapter 2 that for an assessment of roughness the profile must be inspected carefully and a typology be proposed according to the processes, such as turning, grinding, milling and rolling etc., that generate the surfaces. The inspection of the profile graph using different magnifications in the vertical & horizontal directions may be sometimes misleading. This can be seen from Fig. 3.1 that shows the profile of a shaft turned with a feed of 0.1 m.m./rev. with different magnification factors.

Because of such draw backs of experimental observations and specifications derived therefrom, it may be realized that an anlytical description of the profile may prove to be useful. Because of the random characteristics exhibited by all surface profiles, an obvious procedure is to obtain a description based on the probabilistic properties of a random

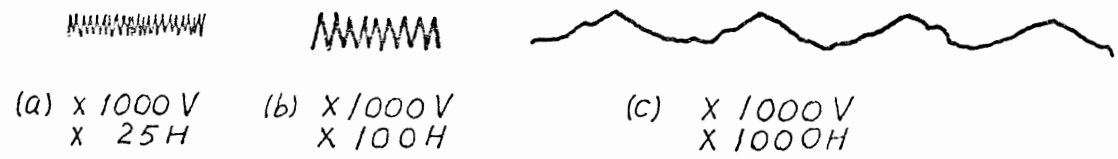

Fig. 3.1 Comparison of different horizontal magnifications.

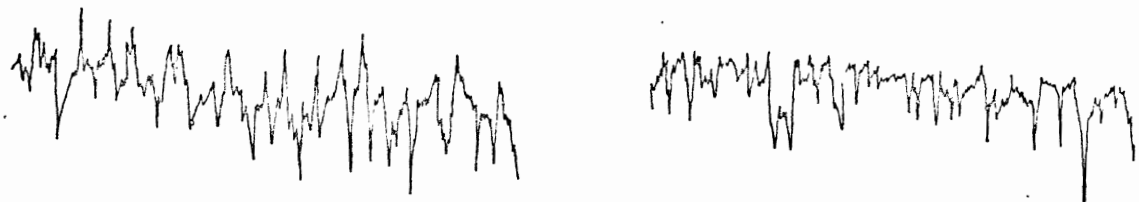

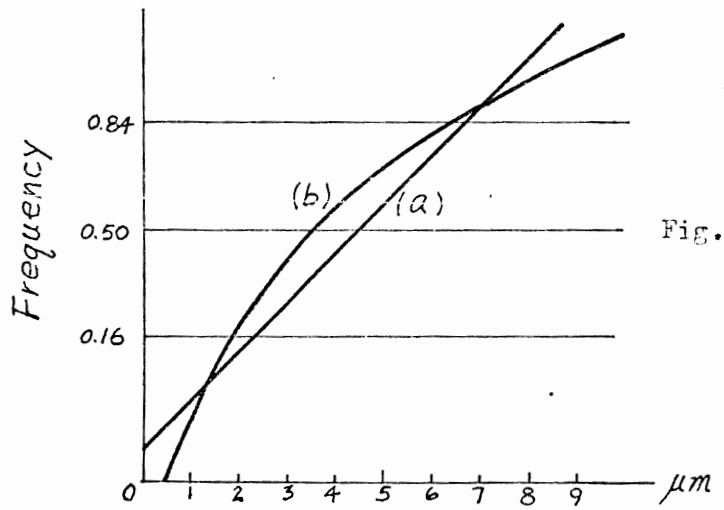

Fig. 3.2 Cumulative probabities for two types of machined surfaces.

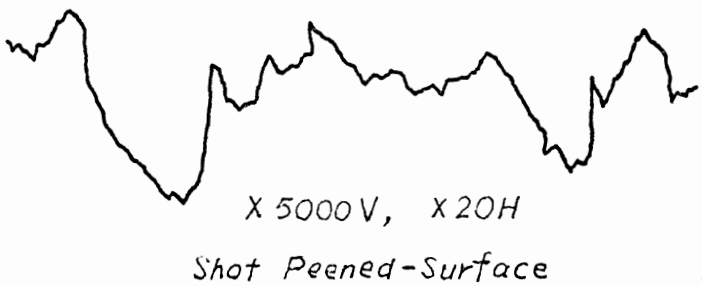

Fig. 3.3 Effect of cut-off on the range of deviation.

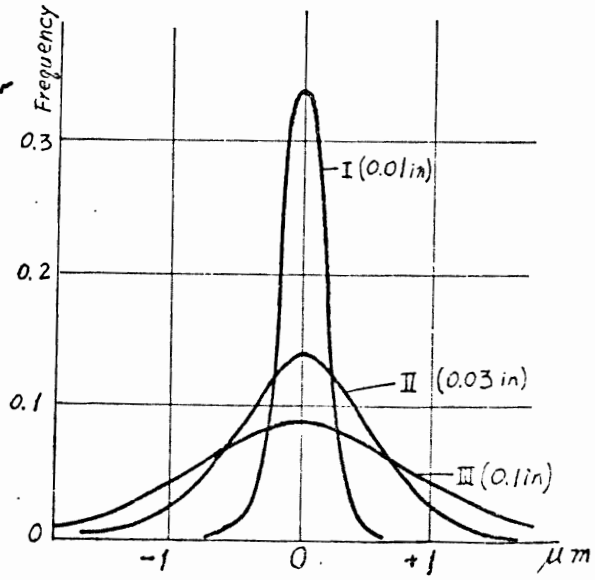

process. A few investigations (11, 12) based on such an approach are available in literature and are presented in detail in the following pages.

3.2 Distribution characteristics:

The shape of the cumulative probability function for a surface is often useful in its description. The profiles of a ground surface before and after lapping are shown in Fig. 3.2 where the curves (a) and (b) indicate the frequency probability against deviation.

Though the profiles of the two surfaces are similar in appearance, the curve (a) shows that a ground surface gives a normal distribution for the cumulative probability, and (b) shows that the lapped one does not.

From the studies carried out in the machine-tool laboratory of ETH (Swiss Federal Institute of Technology), it may be observed that for ground surfaces the distribution is normally Gaussian in nature. The above is also true for shot-peened surfaces. This is illustrated in Fig. 3.3. When different cut-off's I, II, III are used, the character of the distribution does not change, but the range of the deviations changes (see 9, 10).

3.3 Amplitude Density Curves:

A surface texture is generally of arbitrary random type, and hence its description through harmonic analysis alone is not possible. But a better description of the profile can be obtained through simple statistical concepts such as the density of surface amplitudes etc. Such probabilistic measures can be applied regardless of the periodic nature of the profile. The basic definitions normally used in the theory of stochastic processes are now stated.

Consider a random process whose variation with time is as shown in Fig. 3.4. Such irregular variations are also equally true in the case of a surface roughness profile. The amplitude probability is defined by the expression

$$P(y,\ y + \Delta y) = \frac{\sum_{i=1}^{n} \Delta\ t_i}{T} \quad \ldots\ldots\ldots\ldots\ldots\ldots\ldots (3.1)$$

The corresponding amplitude density is then given by

$$p(y) = \lim_{\Delta y \to 0} \frac{P(y,\ y + \Delta y)}{\Delta y} \quad \ldots\ldots\ldots\ldots\ldots\ldots\ldots (3.2)$$

If the value of y is varied from $-\infty$ to $+\infty$, and p(y) is plotted as a function of y, the amplitude density curve can be obtained from the equation (3.2) for the signal under study.

The shape of the amplitude density curve for different types of random signals varies considerably. For a so called normal random process, the amplitude density follows the well-known Gaussian distribution curve as shown in Fig. 3.5. It may be noted that most of the processes in nature are approximately Gaussian.

The probability density curve for a Gaussian random process is

$$p(y) = \frac{1}{\sqrt{2\pi}\ \sigma} e^{-(y - y_o)^2/2\sigma^2} \quad \ldots\ldots\ldots\ldots\ldots\ldots (3.3)$$

where

$p(y)$ = the amplitude density,

σ = the standard deviation, and is equal to $(\langle y^2 \rangle - y_o^{\,2})^{1/2}$,

y_o = the mean value of y given by $\langle y \rangle$,

the angular brackets denoting ensemble average.

For a random signal with a Gaussian distribution following characteristics apply:

(i) A Gaussian distribution is characterized by the two parameters σ and y_o.

(ii) In the case $y_o = 0$, the Gaussian signal is centered around zero as mean.

(iii) The arithemetic average deviation from the mean is

$$Yaa = \int_{-\infty}^{\infty} |y| \cdot p(y)\, dy \qquad \ldots\ldots\ldots\ldots\ldots\ldots (3.4)$$

where $|y|$ is the absolute value of y.

In fact if the record of a signal is studied over a definite time interval T, the probability of finding the amplitude of the signal between levels y and $y + \Delta y$ is given by

$$P(y,\ y + \Delta y) = \int_{y}^{y + \Delta y} p(y)dy = \frac{\sum_{i=1}^{n} \Delta t_i}{T} = \frac{\Delta T}{T} \qquad \ldots\ldots\ldots (3.5)$$

where p(y) is the amplitude density, and $\Delta T = \sum_{i=1}^{n} \Delta t_i$ refering to Fig. 3.4.

The arithmetic average deviation may be deduced as follows.

$$Yaa = \int_{-\infty}^{\infty} |y| \cdot p(y)dy = \lim_{y \to o} \sum_{-\infty}^{\infty} |y|\, P(y,\ y + \Delta y)$$

$$= \lim_{\Delta t \to o} \Sigma |y| \frac{\Delta t}{T} = \frac{1}{T} \int_{o}^{T} |y|\, dt \qquad \ldots\ldots\ldots (3.6)$$

which is the known expression of the average value of a signal. The standard deviation for a Gaussian distribution is given from

$$\sigma^2 = \int_{-\infty}^{\infty} y^2 \cdot p(y)\, dy \qquad \ldots\ldots\ldots\ldots\ldots\ldots\ldots (3.7)$$

Similarly from equation (3.6) it may be deduced that

$$Y_{rms} = \left(\frac{1}{T} \int_{o}^{T} y^2 dt \right)^{1/2} \qquad \ldots\ldots\ldots\ldots\ldots\ldots (3.8)$$

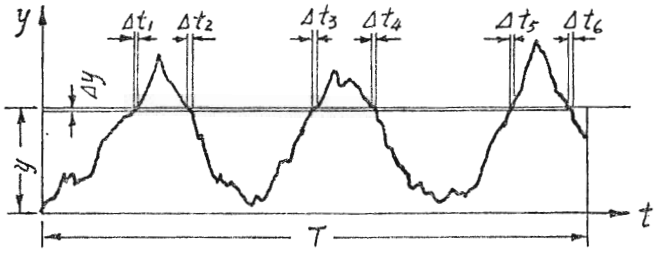

Fig. 3.4 Random signal amplitude versus time.

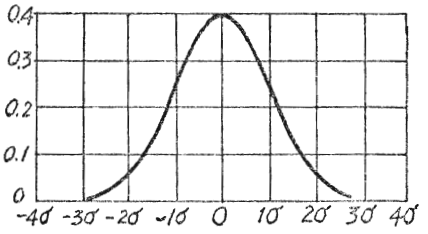

Fig. 3.5 Amplitude density curve of a Gaussian distribution.

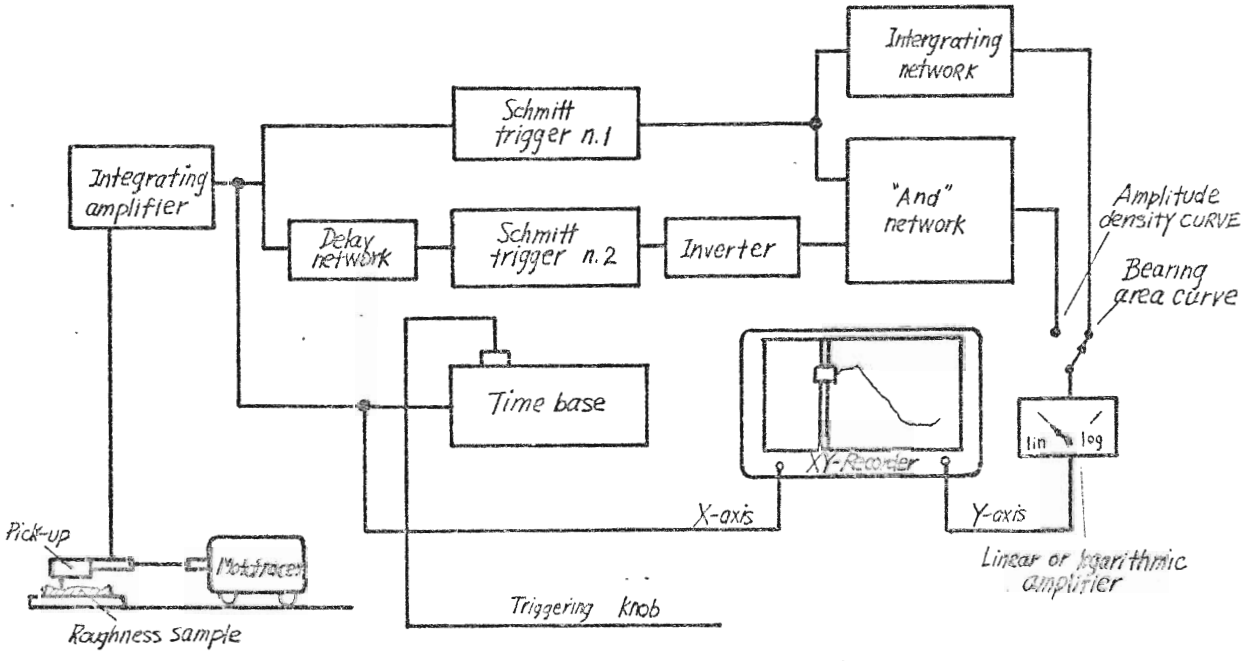

Fig. 3.6 Block diagram for an automatic plotter of the amplitude density curve and bearing area curve.

which gives the widely used root mean square value of any statistical data.

The concept behind obtaining the amplitude density curve is also useful for characterizing the typology of periodically varying profiles, for example sinusoidal, triangular, or square waves, and saw-tooth signals, or any combination of these. In the case of periodic signals only it is sometimes useful to assume that the amplitude density curve is proportional to the time Δt required by the signal for an increase in its amplitude by an amount Δy. In other words, the amplitude density is inversely proportional to the velocity (11) by which the amplitude of the signal changes from y to $y + \Delta y$. That is

$$p(y) = \frac{1}{\frac{dy}{dt}} = \frac{dt}{dy} \quad \text{.....(3.9)}$$

For general cases of profiles, periodic or aperiodic, a method for obtaining the amplitude density curves to a first approximation is through equation (3.2) in the following manner.

If Δy is small, the probability of finding amplitude values of the signal between y and $y + \Delta y$ can be approximately written as

$$P(y, y + \Delta y) \simeq p(y) \Delta y \quad \text{.....(3.10)}$$

By measuring $P(y, y + \Delta y)$ for all values of y and plotting the results, the amplitude density curve of the process under consideration can be obtained. This method is relatively simple but extremely time consuming.

In the field of electro-acoustics, several set-ups have been developed through which the amplitude density curves may be plotted in the laboratory. Fig. 3.6 shows the line diagram of a solid state automatic plotter for the amplitude density and bearing area curves. The mototracer drives the pick-up to travel across the roughness sample

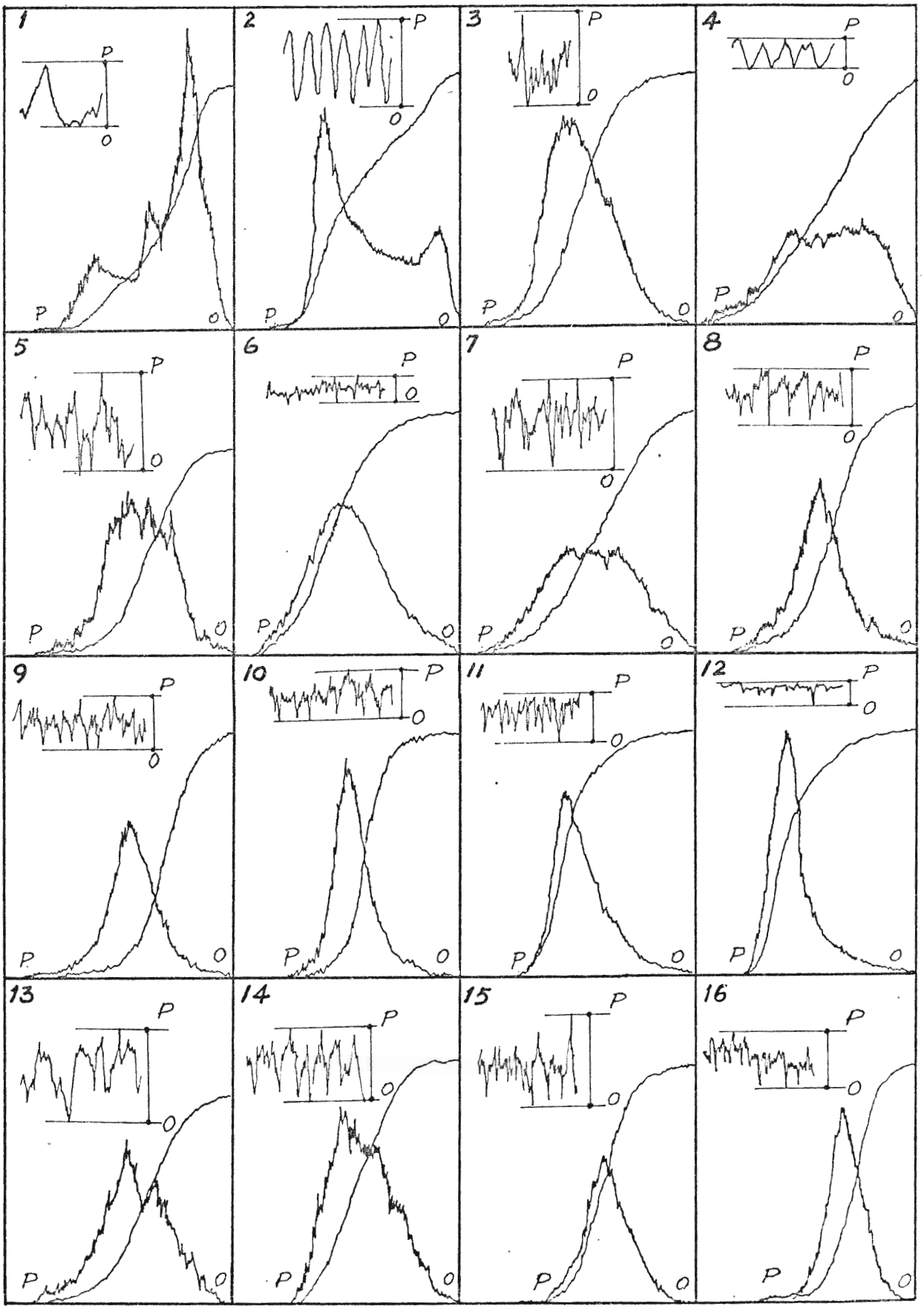

Fig. 3.7 Results of tests on 16 surfaces (11).

and the signals are thus obtained. After amplification, one component is transmitted to actuate the pointer to move in X-direction, and the other component is used to operate the movement in Y direction, which can be selected by a control to plot either the amplitude density curve or bearing area curve. The performance of the automatic plotter is given as follows:

(i) Electronic slit width relative to the amplitude of signal is $\frac{1}{1000}$.

(ii) Plotting time for both the amplitude density and the bearing area curves is 20 seconds.

Results for 16 different samples are shown in Fig. 3.7 and are explained in detail in Table 3.1, Explanation for the 16 test curves (11) shown in Fig. 3.7. In each graph, there are three curves. On the upper left side is the roughness profile, where P indicates the peak, o indicates the bottom of the deepest valley. The lower curve with letters P and o at each end is the amplitude density curve. While the curve extending from lower left side to upper right side is the bearing area curve. For example on the amplitude density curve for super finished surfaces a peak at the left side may be noted which corresponds to the upper part of the profile. This shows acceptable finish for the sample as compared with those of grinding, honing and polishing operations, especially if wear and strength is the criterion for the product. The amplitude density curve corresponding to a running-in process is shown for sample 12. It can be seen that such a process possesses a marked similarity with a super finished surface as far as amplitude density is concerned.

3.4 Other probabilistic descriptions:

In a recent paper, Wallach (12) proposes a quasi-probabilistic method for the description of surface topographies. He considers the

Table 3.1 Explanation for the 16 test curves (11) shown in Fig. 3.7.

Graph No.	Sample Material	Type of heat treatment	Finishing Process	CLA reading, μm.	Vertical Magnification of profile
1	SAE 52100	Annealed	Turning	4	800
2	SAE 52100	Annealed	Turning	5.6	800
3	Brass	Annealed	Diamond Turning	2.25	1600
4	Brass	Annealed	Milling	1.54	400
5	SAE 3310	Annealed	Planing	3.1	800
6	SAE 52100	Hardened	Grinding	.06	20000
7	SAE 52100	Hardened	Grinding (Hard wheel)	1.10	2800
8	SAE 52100	Hardened	Lapping	.62	4000
9	SAE 52100	Hardened	Honing	.6	16000
10	SAE 52100	Hardened	Polishing	.033	20000
11	SAE 52100	Hardened	Superfinishing	.6	800
12	SAE 52100	Hardened	Running-in	.03	4000
13	SAE 1012	Annealed	Forming	1.15	4000
14	SAE 52100	Hardened	Grinding & rolling	.83	2400
15	SAE 52100	Hardened	Sand blasting	1.85	1600
16	SAE 52100	Hardened	Liquid honing	.75	2400

surfaces topography to be made up of a regular waviness plus a random roughness. The former part may be due to the machining marks, warpage, or some particular effect of the manufacturing process. Whereas the latter is due to the random tearing of the material in machining, the chemical or electrolytic attack in non-conventional machining, or any randomness involved in the material removal process.

The regular waviness of the surface may be expressed in the form of a Fourier series and the random roughness is in terms of a probability density function. The calculation of the regular waviness h_w at any point (x, y) on the surface is straightforward. However, the calculation of random roughness h_r is complex and will be explained in detail below. The total height h_t above some reference surface is the sum of the regular waviness and the random roughness. That is,

$$h_t = h_w + h_r \qquad \text{.....(3.12)}$$

where

$$h_w = \sum_{j=o}^{\infty} \sum_{k=o}^{\infty} \left(A_{jk} \operatorname{Cos} \frac{2\pi jx}{Lx} \operatorname{Cos} \frac{2\pi Ky}{Ly} + B_{jk} \operatorname{Cos} \frac{2\pi jx}{Lx} \operatorname{Sin} \frac{2\pi Ky}{Ly} + C_{jk} \operatorname{Sin} \frac{2\pi jx}{Lx} \operatorname{Cos} \frac{2\pi Ky}{Ly} + D_{jk} \operatorname{Sin} \frac{2\pi jx}{Lx} \operatorname{Sin} \frac{2\pi ky}{Ly}\right)$$

and A_{jk}, B_{jk}, C_{jk} & D_{jk} are the Fourier coefficients.

h_r is determined from a cumulative probability distribution for the particular type of surface. Consider the curve for one of the ECM (electro-chemically machined) sample as shown in Fig. 3.8. Here h_r is plotted against the cumulative probability. The value of h_r for any

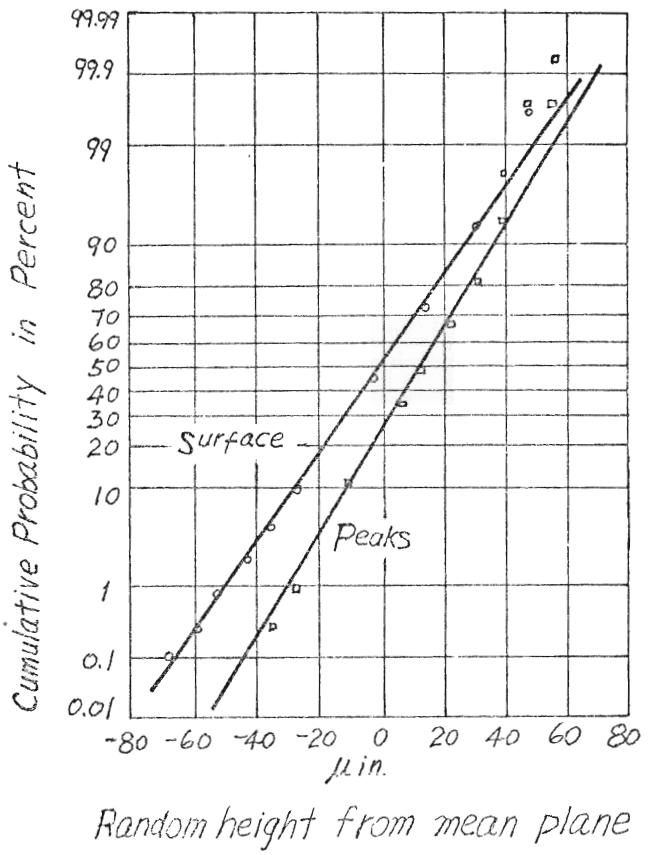

Fig. 3.8 Cumulative probability distribution for an electrochemically machined surface.

point (x, y) is found by following steps:

(i) A table of random numbers with a range of 0 to 100 is prepared.

(ii) From this table a random number is arbitrarily chosen.

(iii) Taking this number as the cumulative probability in percent along the ordinate of Fig. 3.8 a corresponding value of h_r from the graph is read.

(iv) The steps are repeated to cover the other points on the surface following the other random numbers in sequence from the random number table indicated in (ii).

If the cumulative probability distribution can be expressed in terms of an analytical function, then it is possible to obtain a reference plot as the one shown in Fig. 3.8 and proceed as above, or calculate the random height directly from the functional description. In such a case the importance is not in the procedure, but in the ability to express the roughness with a few variables instead of a table or a curve. With the help of such a function it is possible to uniquely describe the random roughness just as it is possible to do for the regular waviness in equation (3.12).

To obtain the Fourier coefficients for the regular waviness h_w and the statistical parameter for the random roughness h_r, it is necessary to start with a three dimensional description of the surface. This is readily done by taking closely spaced parallel traces with a tracer type instrument such as a Talysurf. These traces are generally taken over a small patch of the surface. Each trace is sampled at a constant rate to give a series of equally spaced height readings. The sampling is done so that the traces (series of numbers) can be aligned to give a two-dimensional array of heights. From this array of heights the geometric mean surface is determined. In the case of a nominally flat surface a plane is determined. In the case of a cylinder a mean cylindrical surface

would be determined. All height measurements are then referred to this surface. Then the total surface roughness, h_t, is expressed as a double Fourier series. That is, the Fourier coefficients for equation (3.12) are determined by the regular waviness since the random roughness has no regular components. Actually, in practice only the first few terms in a Fourier series are calculated. This is done for simplification and, in the case of roughness measurements, such an approximation gives reliable results. Thus, the surface roughness seems arbitrarily divided into two components by the number of Fourier coefficients calculated. The decision is really not arbitrary if the results is a regular waviness expressed as a Fourier series and a random roughness expressed as a statistical distribution, and these descriptions are not inconstent with the known way the surface was generated. It is, however, necessary to analyze each surface to decide the cut-off. For more detail, refer to (12).

The method of Wallach is applicable to both conventional and non-conventional maching processes. In comparison with other methods this approach is especially useful in the study of performance of the surfaces prior to their manufacture. Wallach has used this method successfully to calculate the leakage flow between two surfaces by means of a digital computer program.

3.5 Conclusions:

The character of manufactured surfaces is random in nature. Theoretical studies based on probabilistic description have yielded some applicable approaches. Among these, the amplitude density curve method possesses the advantage to lend itself to the employment of an automatic plotter, by which the density curve and the bearing area curve can be obtained at the laboratory. Such a method provides some criteria for the evaluation of wear resistance as well as load carrying capacity . The method

developed by Wallach can be used to calculate the performance of surfaces, such as leakage between surfaces etc., prior to manufacture. All the parameters for the description of the correlation between the surface texture and its physical and mechanical properties have not been completely understood, and investigations using the theory of stochastic processes are still underway.

Research is continuing at Sir George Williams University, on the best description of a surface profile using experimental and analytical techniques. An automatic computerized method to get all the stochastic descriptions such as probability density, auto-correlation, spectral density from measured data has been developed. Also being carried out by the same team is a representation of texture through two separate variables based on amplitude fluctuations and probability of valley intercepts using methods of random excursion employed in Communication engineering.

CHAPTER 4

SURFACE ROUGHNESS AND FATIGUE STRENGTH

4.1 Introduction:

Components made of the same material but produced by different manufacturing methods will have different fatigue strengths, even though their roughness numbers are the same. The main reason for this is due to the fact that the residual stresses on the surface layers are not of the same nature.

The origin of residual stresses can be generally attributed to

(i) plastic deformations from non-uniform thermal expansion or contraction,

(ii) volume changes from chemical reactions, precipitation or phase transformation,

(iii) mechanical working.

Residual stresses are beneficial if they are compressive and detrimental if tensile, particularly in the cases of material hardened by working or by heat treatment. The following typical processes normally cause residual stresses (see 14, 15, 16):

(i) Tumbling - causes compressive residual stresses, has a good influence on the fatigue limit..

(ii) Vapor blasting and shot peening - introduces favorable compressive residual stresses.

(iii) Grinding - mainly thermal residual stresses reproduced, volume changes due to phase transformation and cold work.

(iv) Worn cutting tools - tends to generate tensile residual stresses.

(v) Electric Discharge machine - produces tensile residual stresses.

(vi) Mechanical treatment - glass bead peening, surface rolling, honing, polishing etc., all cause compressive residual stresses.

4.2 Influence of finishing processes:

Many investigators who studied the effect of surface finish on fatigue strength did not utilize precise measurements of surface roughness. Usually the surface finish was designated by the method used for the preparation of the test specimens. Moore and Kommers (17) investigated the effects of surface finish on fatigue strength of two carbon steels with five grades of surface finishes. Their results are given in Table 4.1, Sample conditions used in the endurance limit test.

A high polish is seen to increase the endurance limit slightly above that for a standard polish, while the rough surfaces reduce the endurance limit 10 to 15 percent. Similar results were obtained by Thomas (18) which are also listed in the last column of Table 4.1.

In a recent study, Siebel and Gaier (19) found that there is a critical surface roughness beyond which there is no increase in fatigue strength with a decrease in surface roughness. This critical roughness is independent of the type of fatigue stress but varies with the material and the metallurgical structure. They used the maximum depth of groove as the criterion for classifying surface roughness rather than the root mean square value. For steels tempered to relatively high strength, the critical roughness value is 1 to 2 microns (40 to 80 micro-inches). For annealed steels, the critical roughness value is 4 to 6 microns. Once the critical roughness is exceeded, there is a linear drop in fatigue limit with the logarithm of the depth of roughness.

From the view point of fatigue of metals, it is generally most desirable to have the longitudinal axis of the final irregularities and surface scratches running parallel to the direction of principal tensile stress.

Table 4.1 Sample conditions used in the endurance limit test (17, 18).

Type of surface finish	Moore & Kommers (17), Rotating beam, .02% carbon steel, annealed		Moore & Kommers (17), Rotating beam, .49% carbon steel, quenched and drawn.		Thomas (18), Rotating cantilever, .33% carbon steel.	
	Endurance limit psi.	% of standard polish	Endurance limit psi.	% of standard polish	Endurance limit psi.	% of standard polish
High polish, long.	50,500	103			41,500	102
Standard polish	49,000	100	26,000	100	40,500	100
Coarse emery					39,000	100
Ground	45,000	93				
Smooth file					38,500	95
Smooth turned	43,000	88	24,000	92	36,500	90
Rough turned	41,500	85	23,000	88		
Bastard file					35,500	88

Any scratches or "furrows" perpendicular to the direction of tensile stress may serve as a nucleus or stress concentrator to initiate a fatigue fracture. Caswell (20) concluded from tests on a mild steel, that grinding and polishing in direction transverse to the axis of principal stress gave an endurance limit about 26 percent lower than for grinding and polishing in the principal stress direction.

The influence of surface roughness on the fatigue life of SAE 1035 and SAE 3130 steel was studied by Fluck (21). Six methods of surface preparation were used and groups of 12 similar specimens were tested at two stress levels for each of the two steels. Results are shown in Table 4.2, Results of test to evaluate the effect of surface roughness on the fatigue life of steel.

The fatigue life is noticed to be greatly increased by methods of surface preparation which reduce the size of circumferential scratches (longitudinal roughness measurement). Longitudinal scratches, even though large, have very little influence on the fatigue life. The manufacturing process affects not only the surface roughness but also the surface hardness, and this in turn has a definite effect upon fatigue strength. Investigations by Cina (25), and by Sinclair, Corten and Dolan (26) indicate that this increase in hardness (from cold working the surface) may be even more important than the surface roughness in influencing the fatigue strength.

Cina (25) investigated extensively the effect of surface conditions upon fatigue strength. He considered that while final polishing of a fatigue specimen is carried out to reduce the surface roughness from previous turning or polishing operations, this polishing with emery paper may produce cold working of the surface, the effect of which may be to

Table 4.2 Results of test to evaluate the effect of surface roughness on the fatigue life of steel (21).

Type of finish	SAE 1035 Specimens				SAE 3130 Specimens			
	Surface roughness in micro-in.		Median fatigue life	Quartile scatter factor	Surface roughness in micro-in.		Median fatigue life	Quartile scatter factor
	Long.	Circ.	Cycles	%	Long.	Circ.	Cycles	%
	Unit stress 38,000 psi.				Unit stress 95,000 psi.			
Lathe formed	65	18	258,000	24	105	15	24,000	43
Partly hand polished	16	19	728,000	12	6	4	91,000	20
Hand polished	6	10	790,000	24	5	3	137,000	27
Ground	13	95	836,000	28	7	45	217,000	19
Ground & polished	3	6	1,260,000	44	2	6	234,000	47
Superfinished	8	7	848,000	19	7	8	212,000	46
	Unit stress 36,000 psi.				Unit stress 88,000 psi.			
Lathe formed	65	18	566,000	10	105	15	54,000	24
Partly hand polished	16	19	1,555,000	19	6	4	280,000	27
Hand polished	6	10	1,670,000	25	5	3	311,000	61
Ground	13	95	3,598,000	51	7	45	368,000	24
Ground & polished	3	6	3,365,000	195	2	6	690,000	77
Superfinished	8	7	1,822,000	16				

Table 4.3 Results of test to evaluate the effect of surface roughness on the fatigue strength of steel (25).

Type of steel	Fatigue strength tons/in^2		Effect on finite fatigue life
	Mechanically polished	Electrolytically polished	
13% chromium fully martensitic	50	46.5	Considerable
13% chromium tempered martensitic	35	29	Slight
20% chromium fully softened - ferrite	19	15	Slight
25/20 chrome nickle fully softened austenite	19	15	Negligible
9/3/8/.6 Mn-Cr-Ni-C Stable austenite softened	24	18	Negligible
18/8 Nickle chrome unstable austenite	19	17	Negligible
Low alloy (3% Ni) tempered martensite	29	24.5	Negligible

increase the fatigue strength. He carried out several tests on steel and the results are given in Table 4.3, shown above. It may be seen that the fatigue strength of mechanically polished specimens are higher than the electrolytically polished, and their effect on fatigue life varies from considerable to negligible. Further to show that mechanically polished specimens have longer fatigue life and higher fatigue limit due to cold work introduced into the surface, Cina (25) stress-relieved a set of identically heat treated low alloy rotating-beam fatigue specimens and blanks in a vacuum. The blanks were then machined and polished. Fatigue tests of these specimens showed that the fatigue strength was reduced

from 29 to 24.5 tons per square inch by stress relieving which is the same reduction that was obtained for the electro-polished specimen. From the results of his tests, Cina (25) drew the following hypothesis: Mechanical polishing results in artificially greater fatigue strength due to cold effects introduced into the surface of fatigue specimens, while electro-polishing gives truer fatigue strength value since it reveals a true virgin surface of the material.

Sinclair, Corten and Dolan (26) performed the similar tests on the fatigue strength of two titanium alloys and is useful in application to actual srevice conditions. A summary of their results is given in Table 4.4. For electro-polished specimens series 3, .002 in. was removed from the surface of mechanically polished specimens, and for series 8, .010 in. was removed from the surface. Here, it is found that, in general, the fatigue strength varied according to the hardness of the surface layer, with the highest hardness corresponding to the greatest fatigue strength. Roughness of the surface is found to influence fatigue strength but to a much lesser degree than hardness. The loss in fatigue strength due to surface roughness becomes greater at high surface hardness. As a first approximation, the relationship between surface hardness, surface roughness, and fatigue strength from the data given may be expressed through the equation

$$Z = 207\ X^{-.0284}\ Y^{1.017} \qquad \text{..... (4.1)}$$

where Z is fatigue limit, p.s.i.

X is root mean square surface roughness,

and Y is Knoop surface hardness (100 gram load).

This equation (26) indicates that surface roughness does not seriously

Table 4.4 Summary of results of tests by Sinclair et al (26).

Material	Series	Description	Stress concentration factor.	Average roughness rms, micro-in.	Surface hardness 1000 gr. Knoop.	Fatigue limits, 1000's of psi.				No. of specimens used in staircase analysis.
						Mean value of fatigue limit.	95% Confidence limits	Calculated from equation (4.1).	Experimental value minus calculated value.	
RC 130B Ht 1	1	Mechanical polish		7	455	87	4	99	-12	13
	2	Cold rolled 15-lb.		13	480	103	3	103	0	12
	3	Electropolished		3	445	91	2	99	- 8	13
	4	Notched cold roll	2.02			64	1			14
	5	Ground surf.		40	345	66	3	71	- 5	16
	6	Ground notch	2.02			36	2			16
	7	Ground V notch	2.7			26	3			14
	8	Special electropolish		3	365	79	2	81	- 2	11
RC 130B Ht 2	1	Mechanical polish		7	385	88	5	83	5	13
	10	Cold roll scratch		35	430	89	5	89	0	13
	11	Cold roll 30-lb.		25	450	100	3	94	6	13
	12	Cold roll 40-lb.		7	480	111	5	104	7	19
	13	As machined		155	470	86	2	94	- 8	10
Ti 140A	1	Mechanical polish		7	395	90	5	86	4	17
	2	Cold rolled 15-lb.		10	410	98	3	88	10	13
	3	Electropolished		3	375	79	16	83	- 4	16
	4	Notch cold roll	2.02			67	3			13
	5	Ground surf.		40	370	81	1	76	5	9
	6	Ground notch	2.02			38	2			14
	7	Ground V notch	2.7			30	1			14
	9	Mech. polish scratch		26	350	71		73	- 2	14
	11	Cold roll 40-lb.		25	450	97	2	94	3	14

influence the fatigue strength of these alloys, and for constant values of surface roughness the relationship between fatigue limit and surface hardness is approximately linear.

4.3 Design criteria:

As an aid to machine designers, Noll and Lipson (22) plotted curves of endurance limit versus tensile strength, using the data obtained by numerous investigators for ground, machined, hot-rolled and as-forged (with no other treatment after forging) specimens, and are illustrated in Fig. 4.1. All data from ground, honed, lapped and superfinished specimens are included in the ground surface category. Similarly, all machined specimens, whether rough or finish machined, are included in one category, and the curve has been extrapolated because of the limited data available. These data have also been corrected for the effect of size of the specimen before used in the plot (see 22).

Using average curves, like for Fig. 4.1, as a basis for predicting "infinite" life (the endurance limit) for the products and employing an empirical relationship between tensile strength and Brinell hardness for steel, charts for design purposes are constructed based on a modified Goodman diagram. The maximum applied stress is plotted against the mean stress of the loading cycle for specific ranges of Brinell hardness, for ground, machined, as-rolled and forged surfaces. Fig. 4.2 shows some typical curve. Though called working stress by Noll and Lipson, it may be observed that charts are set up to delineate conditions that result in fracture and have not been reduced by a "Factor of safety". Eighteen similar curves covering a Brinell hardness range from 160 to 555 are also proposed by these authors (22).

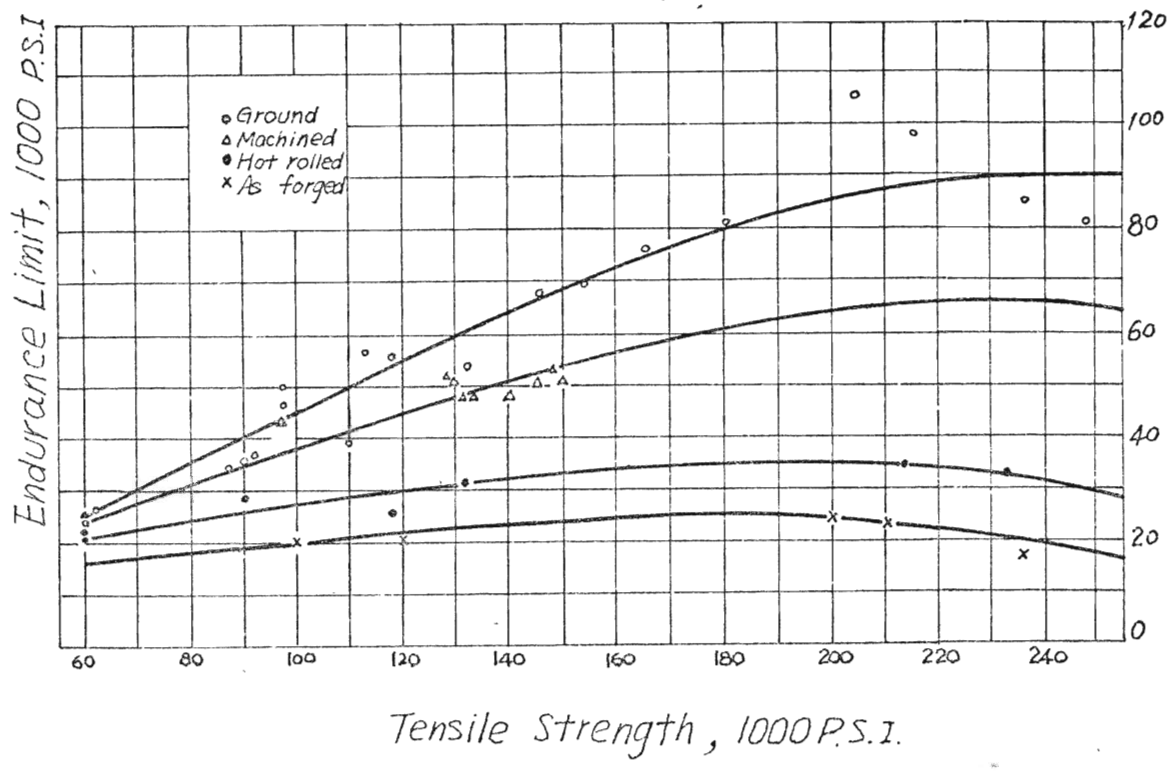

Fig. 4.1 Relation between endurance limit and tensile strength for specimens with different machined surface finishes.

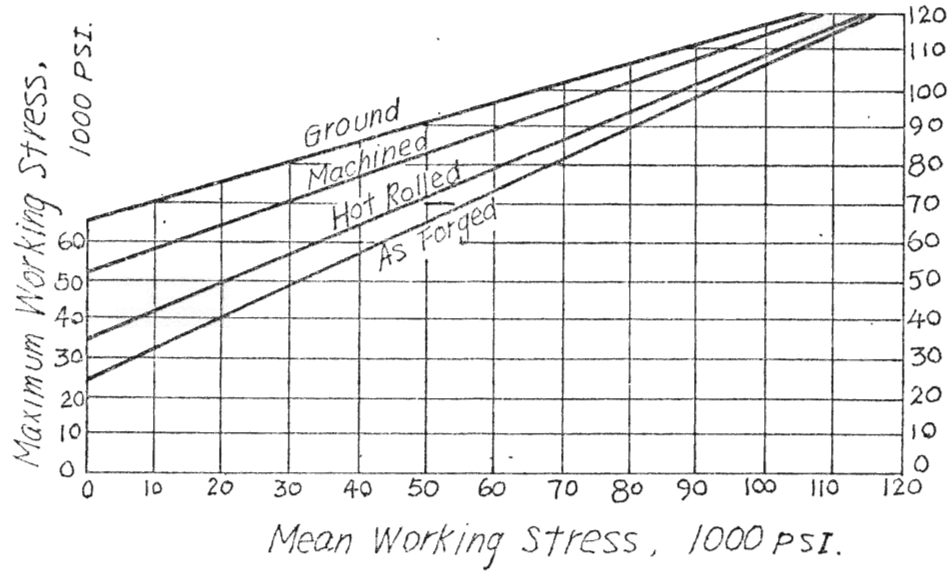

Fig. 4.2 Relation between maximum and mean stresses at endurance limit for parts having Brinell hardness 302-321.

For use under conditions where less than a million overload cycles may be encountered in steel components during normal life, Noll and Erickson (23) constructed charts for critical stresses against a given "finite life". The same hardness ranges as those in the curves referred in Fig. 4.2 are used, the stresses and the corresponding finite life from the upper portions of the available stress-life curves are used in constructing these curves. Fig. 4.3 shows the design plot valid for the Brinell hardness range of 302 to 321. However, a check with the results obtained by Fluck (21) for SAE 3130 with a Brinell hardness of 285 shows that the machined specimens have approximately 500 % longer median life and the ground specimens have approximately 1200 % longer median life than those predicted by Noll and Erickson's chart (see 23).

A series of tests carried out by Gunn (24) gives the following fatigue strength reduction factors K_f for Alluminium alloy D.T.D.363, where

$$K_f = \frac{\text{Unnotched fatigue strength}}{\text{notched fatigue strength}} \quad \text{at some specific endurance limit.}$$

Longitudinal polish	5.5 micro-inches,	K_f = 1.0 at 10^7 cycles,
Circumferential polish	9 micro-inches,	K_f =1.06 at 10^7 cycles,
Fine machine	64 micro-inches,	K_f =1.12 at 10^7 cycles,
Rough machine	100 micro-inches,	K_f =1.16 at 10^7 cycles.

For materials used in aircraft structures, a value of K_f equalling 3 to 5 are common and values of 8 to 9 can occur. When two or more stress concentrations act simultaneously they are considered to be communicative. Therefore, for an average K_f of 4, changing from 64 micro-inches finish to a 9 micro-inches finish would result in a small change of K_f from

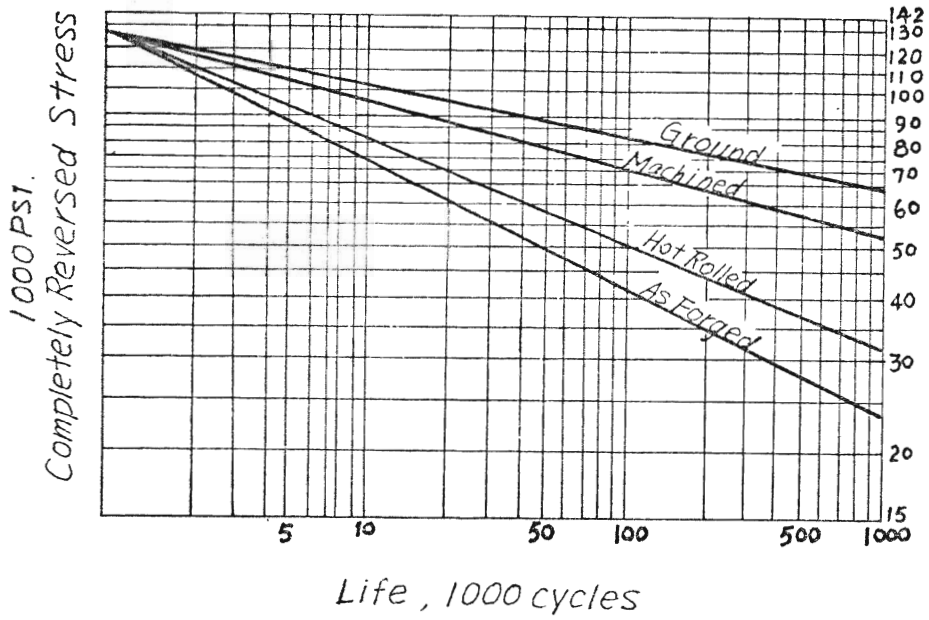

Fig. 4.3 Allowable stresses for limited life for parts whose minimum Brinell hardness lies between 302-321.

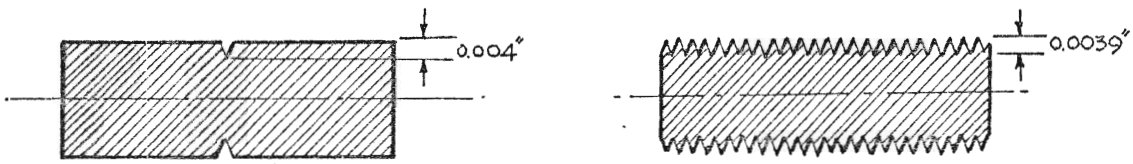

Fig. 4.4 Two identical pieces tested for fatigue, one having a single sharp groove, the other having been rough turned.

4.48 to 4.24. This is insignificant when one considers the inherent scatter in fatigue results (see 24).

4.4 Effect of surface flaws:

Surface blemishes or flaws may be due to isolated scratch marks or notches which affect the roughness value of the surface only a little but can have a very drastic effect on the fatigue strength of the component.

The example reported by Moore and Kommers (24) illustrates how the roughing up of a surface to the deepest scratch mark improves the fatigue resistance. As shown in Fig. 4.4 two identical test pieces are lapped to the same initial roughness values. In one test piece a single sharp groove .004 in. deep is cut and the other is rough turned to a maximum depth of .0039 in. Both test pieces are subjected to fatigue tests and the first sample with a single groove showed a reduction of 80% of fatigue strength, whilst the second showed a reduction of only 11%.

The most important consideration for all components with regard to fatigue is the surface condition (irregularities outside the roughness pattern range). It is essential that machining operations produce a residual stress field that will prevent crack initiation or retard or stop crack propagation and this stress field should not be disturbed by individual deep scratch marks. These conditions, however, bear little relation to their measurable surface texture (see 24).

4.5 Surface treatment:

Under axial loading the surface condition does not play as prominent a part in determining the fatigue strength of the member as it does for a condition where a high stress gradient exists with peak stresses occuring at the surface. However, in all cases employing tests by axial loading, it is found that surface stresses are usually somewhat higher than those

in the interior. For a metal part with an intentional surface layer, endurance limit may be determined more by the characteristics of the outer surface layer than by mechanical properties of the base metal.

Among surface treatments which markedly affect the fatigue strength are: nitriding, carburizing, flame or induction hardening, shot peening, sand blasting and cold rolling. Several of these treatments may reduce or minimize the harmful effects of stress concentration arising from rough surface finish. It is generally believed that the beneficial effects are due to the compressively prestressed casing introduced on the surfaces by these treatments. The applied stresses are therefore counteracted to some extent by the existing residual compressive stresses. Furthermore, because even the most highly polished surface has microscopic notches, the layer adjacent to the surface is stronger in resisting fatigue than the same metal without the case protection.

Several investigators have proved that the endurance limit of nitrided steel is increased from 20 to 40% above that for polished specimens of unnitrided steel. Case carburizing for increasing surface hardness may also be used to improve the endurance limit of a machine part. But carburized surface is brittle or notch sensitive, and damaging cracks may readily form during quenching especially in an irregularly shaped part. A decarburized surface on the contrary markedly reduces the fatigue strength. Austin (27) reports a 20% decrease in endurance limit of a 0.38 percent carbon steel with decarburization of the surface.

Harger (28) reports that the fatigue strength may be increased by induction and flame hardening. However, Wiegang (29) establishes that fatigue fracture often occurs in the region of transition from

the hardened layer to the base metal. Data is not presently available on the effect of surface finish in relation to these treatments, but if the failure does not originate in the surface, a moderate roughness of the surface may not be expected to have a measurable influence.

A perfectly smooth surface is not necessarily the best one to resist fatigue. Shot peening has become popular in many instances for increased fatigue resistance and it also has the advantage of eliminating careful polishing or machining after heat treatment and may serve as a means of cleaning or descaling. Results of Wiegand (29) indicate that the fatigue strength of a shot-blasted rough surface is about equal to that of ground and polished (not shot-blasted) one. Zimmerli and Lüppert (30) find that usage of smaller sized shots in the process gives a greater endurance limit. They also find that fatigue strength increases with peening time up to certain optimum value. Excessive peening intensity may cause a decrease in the fatigue strength.

Cold rolling of steel improves the fatigue strength in the same manner as shot peening. Surface roughness of a highly polished part can be somewhat increased by cold rolling, but the endurance limit in reversed bending is also increased.

4.6 Conclusions:

Turned or filed specimens have a fatigue strength 10 to 25 % below that of standard polished specimens. Surface treatments, such as nitriding, carburizing, and cold working, can increase the fatigue strength considerably. The higher the hardness of the material, the greater the effect of surface roughness in reducing the fatigue

strength of nontreated surfaces. All methods of surface preparation, however, except electropolishing, cold work the surface and affect the hardness and accompanying residual stresses at the same time as they produce a characteristic surface roughness. The fatigue strength is influenced by all the factors mentioned in this Chapter and not just by surface finish alone.

CHAPTER 5

INFLUENCE OF SURFACE ROUGHNESS ON ACHIEVING DESIRED LUBRICATION

5.1 Introduction:

When two surfaces are kept apart by a film of lubrication contact from time to time is bound to occur if the surfaces are not perfectly flat. According to Bowden and Tabor (31) and other works on this subject (4, 37, 38), the wear is caused in the following steps:

(i) fluid oil film supporting,

(ii) boundary lubrication (mono-molecular film),

(iii) oxide film supporting,

(iv) films of phosphides, sulphides or metallic soaps supporting,

(v) metal to metal contact,

(vi) local welds and shears (often accompanied by the plucking of wear particles out of the weaker surface).

The final run-in surfaces will distinctly differ both geometrically and physically from their initial conditions depending on the requirements of their ultimate performance. That is, they cannot be precisely simulated by any preparatory manufacturing processes. As all moving parts are supported by bearings which have different requirements for lubrication, therefore the study of the influence of surface texture on the lubrication becomes an important problem in mechanical engineering. On this topic numerious experimental and analytical works have been done in the past and a few of them will be discussed in this Chapter.

5.2 Experimental results and deductions:

The graph shown in Fig. 5.1 gives the set-up and test results obtained by Spragg (5) of the Taylor Hobson Laboratory, in which a

cathode ray oscilloscope is used to display the behavior of a small alternating voltage (50 millivolts from 50 cycle mains) applied across the bearing surfaces. Here the relation of the coefficient of friction to a dimensionless parameter ZN/P is shown. The terminology for this parametric description is given by the following:

Z= viscosity of the lubricant,

N = the speed,

P = the load per unit projected area of the bearing.

From the plot it is seen that at least in some cases, if not all, the toe of curves corresponds to the transition from a fluid film to a boundary layer lubrication.

In Spragg's set-up, the thickness of oil film δ T becomes less as the speed is reduced until the high spots of the surfaces begin to come in contact. Then flashes from the sine wave in the oscilloscope towards the horizontal axis of the screen appear, and increase in number as the speed is further reduced. Finally when the contact is continuous the flash point in the oscilloscope moves in a straigth line across the screen. Thus to the left of the toe in the curves in Fig. 5.1 there is a continuous contact causing a rise in friction coefficient (defined as the ratio between the driving force F and the load P, i.e. μ = F/P) as the speed falls due to the processes of boundary layer and metallic shear coming successively into play. To the right of the toe, the surfaces are held apart by a fluid film, the thickness of which tends to increase with an increase of speed. The apparent increase in the value of the coefficient of friction, μ , in this region is perhaps accounted for by the increasing amount of work required to overcome the viscous

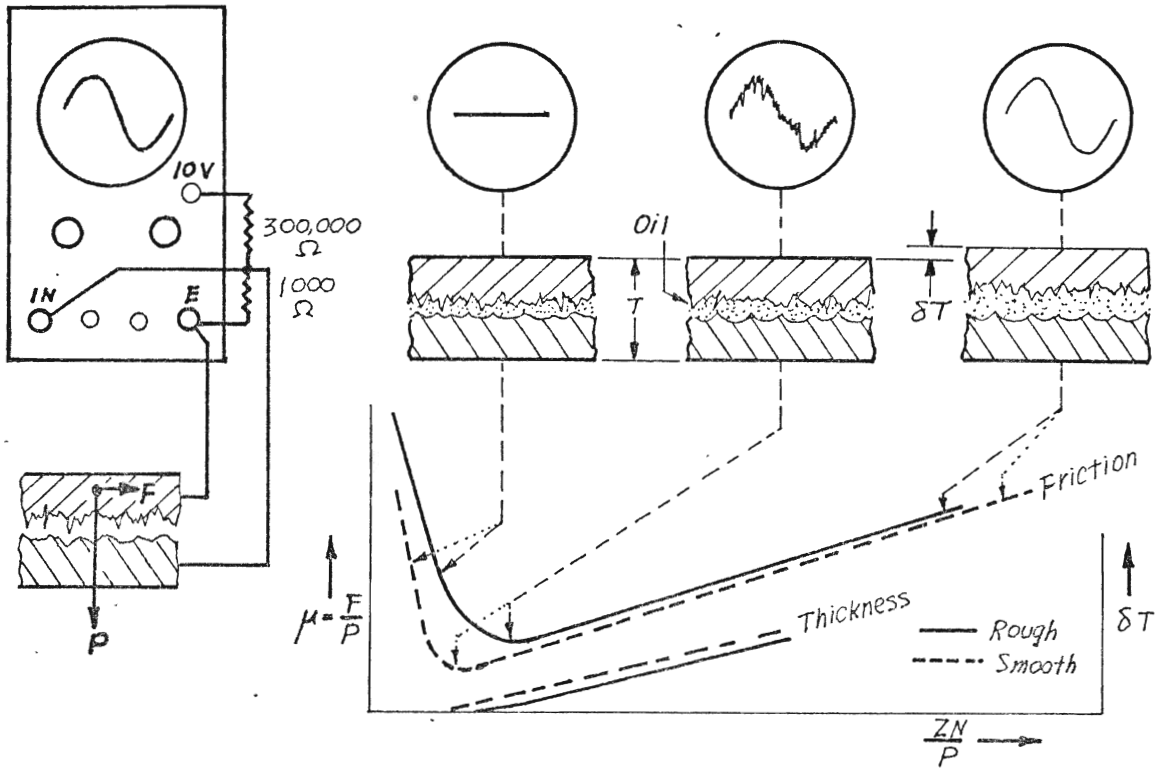

Fig. 5.1 Functional effect of primary texture in bearings.

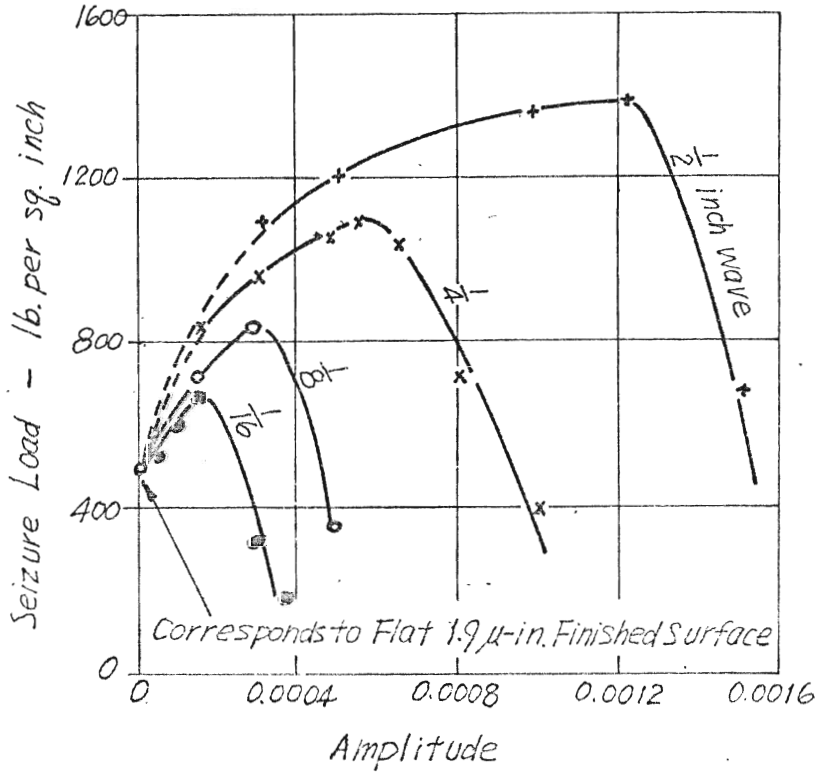

Fig. 5.2 Effect of waviness on thrust bearing capacity.

drag of the oil film.

If the primary texture is reduced in height, the toe of the curve will move towards the origin and become sharper, as shown by the dotted lines in the graph (5). This is because the average thickness of the fluid film has reduced before the high spots of the surfaces engaged. Improved finish, therefore, permits lower speeds or higher loads before this stick-slip region is entered according to Wright Baker (5).

From the results presented above one may conclude that all sliding surfaces should start with as fine a finish as possible. In practice this is not always the case, because often there are other considerations that must be taken into account. In the case of aero-engine cylinder, for example, too fine a finish permits the build-up of an excessively thick oil film, and a definite roughness, produced by a series of carefully controlled processes, is essential to satisfactory performance (4). Furthermore, if local seizure does occur, the result is likely to be more serious with very smooth than with rougher surfaces, partly because weld particle that may be detached, or any dirt in the oil, has further distance to travel before it finds a place where it can lodge, and partly because protective oil will also have to travel farther before it can reach the affected spot. Yet, scratch marks having a favourable direction (lay), especially criss-cross patterns, can be helpful in distributing the oil over the surfaces. Again, if there are initial errors of form and bad alignments, very smooth surfaces may take longer run-in period than those that are not as smooth, except running into a risk of scuffing.

The secondary texture of the surface is also vitally important due to the fact that it plays a role in building up oil wedges. Some results for a 7 inch diameter flat thrust bearing obtained by Samala (32) using a set-up designed at the Manchester College of Technoligy are shown in

Fig. 5.2. Waves of about ½ in. circumferential pitch and .0013 in. height artificially lapped on one of the members increased the permissible load by a factor of about 3. In other words the toe of the μ versus ZN/P curve on Fig. 5.1 was moved towards the origin, affecting it in the same way as a refinement in the primary texture.

5.3 Effect of slider lubrication-An analytical approach (44):

In a paper on the effect of surface roughness on slider bearing lubrication by Tzeng and Saibel (44) the combined effect of waviness and roughness is considered as a Beta distribution. In this work an analytical treatment based on the above mentioned description for the random surface roughness is presented and using an example the order of magnitude of the frictional effects produced are demonstrated.

Consider a wide slider bearing as shown in Fig. 5.3 in which the change of oil pressure, $\frac{dp}{dz}$, along the width is negligible. The Reynolds equation for incompressible lubrication flow (41) is then reduced to

$$\frac{d}{dx}\left(H^3 \frac{dp}{dx}\right) = \Lambda_1 \frac{dH}{dx}, \qquad \ldots\ldots\ldots\ldots\ldots\ldots (5.1)$$

where $p = p(x)$ is the pressure,

$H = H(x)$ is the film thickness,

μ is the viscosity of the lubricant (constant),

and $\Lambda_1 = 6\mu U$, U being the velocity of the slider.

A simple integration of equation (5.1) yields

$$\frac{dp}{dx} = \frac{\Lambda_1}{H^2} + \frac{\Lambda_2}{H^3}, \qquad \ldots\ldots\ldots\ldots\ldots\ldots (5.2)$$

here Λ_2 is an integration constant.

Let ϵ denote the random roughness deviation from the mean bearing surfaces, and h(x) the nominal film thickness defined by the mean surfaces. Then one can write

$$H(x) = h(x) + \epsilon \ .$$

If the right hand side of equation (5.2) is treated as the input stochastic process, the pressure distribution p(x) can then be regarded as the stochastic output of a linear system. The output process must satisfy two boundary conditions at the ends, namely

$$p(0) = 0 \text{ and } p(\ell) = 0, \quad \ldots\ldots\ldots\ldots\ldots\ldots\ldots\ldots (5.3)$$

at $x = 0$ and $x = \ell$ respectively.

Let random roughness variable ϵ be characterized by its probability density function $f(\epsilon)$. Taking the expected values of the terms in equation (5.2),

$$\frac{d\langle p\rangle}{dx} = \left\langle \frac{dp}{dx} \right\rangle = \Lambda_1 \left\langle \frac{1}{H^2} \right\rangle + \Lambda_2 \left\langle \frac{1}{H^3} \right\rangle \quad \ldots\ldots\ldots\ldots\ldots (5.4)$$

with corresponding boundary conditions

$$\langle p(x) \rangle_{x = 0} = 0, \ \langle p(x) \rangle_{x = \ell} = 0 \quad \ldots\ldots\ldots\ldots\ldots\ldots (5.5)$$

to be satisfied. The symbol $\langle\ \rangle$ represents ensemble average or the expected value. Noticing that the terms on the right hand side of equation (5.4) are expected values of functions of the random variable ϵ, it may be shown that

$$\left\langle \frac{1}{H^n} \right\rangle = \int_{-\infty}^{\infty} \frac{f(\epsilon)}{(h + \epsilon)^n} \, d\epsilon \ , \ (n = 2, 3). \quad \ldots\ldots\ldots\ldots\ldots\ldots (5.6)$$

Upon determination of the right hand side of equation (5.4) using equation

(5.6), the expected value of the pressure as a function of x is obtained by solving this differential equation. Symbolically

$$\langle p(x)\rangle = \Lambda_1 \int_0^x \left\langle \frac{1}{H^2} \right\rangle dx + \Lambda_2 \int_0^x \left\langle \frac{1}{H^3} \right\rangle dx. \quad \ldots\ldots\ldots\ldots (5.7)$$

The integration constant Λ_2 can now be determined by the second condition in equation (5.5). Integrating the final expression for $\langle p(x)\rangle$ over the bearing surface area, the expected value of the total load-carrying capacity per unit width becomes

$$\overline{W} = \int_0^\ell \langle p(x)\rangle \, dx. \quad \ldots\ldots\ldots\ldots\ldots\ldots\ldots\ldots (5.8)$$

Based on the same assumptions and reasoning as before, the shearing stresses are given by (see 33)

$$\tau_1 = -\frac{\mu U}{H} - \frac{H}{2}\frac{dp}{dx} \quad \text{on the shoe,} \quad \ldots\ldots\ldots\ldots (5.9)$$

$$\tau_2 = -\frac{\mu U}{H} + \frac{H}{2}\frac{dp}{dx} \quad \text{on the slider.} \quad \ldots\ldots\ldots\ldots (5.10)$$

Here $\frac{dp}{dx}$ can be replaced by equation (5.4). The expected value of the total frictional force may likewise be obtained as

$$\overline{F}_1 = \int_0^\ell (\tau_1)\, dx, \quad \ldots\ldots\ldots\ldots\ldots\ldots\ldots\ldots\ldots (5.11)$$

$$\overline{F}_2 = \int_0^\ell (\tau_2)\, dx. \quad \ldots\ldots\ldots\ldots\ldots\ldots\ldots\ldots\ldots (5.12)$$

Consider now a plane-slider bearing of infinite width. Let the roughness of the bearing surfaces be represented by a Beta density function of the form

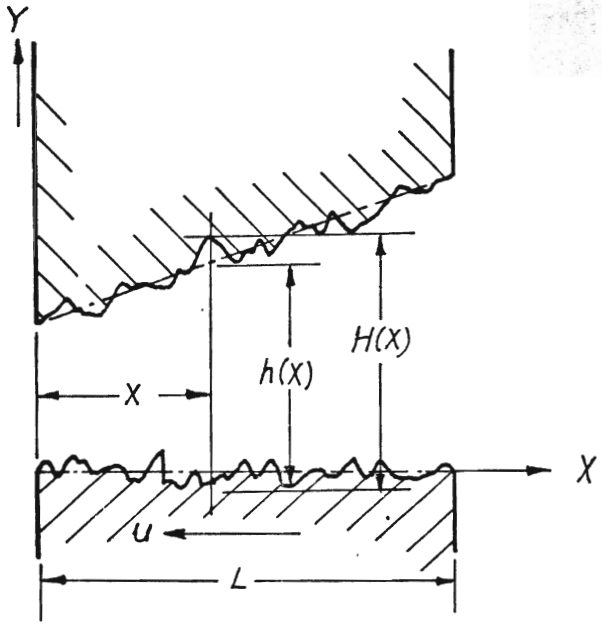

Fig. 5.3 Slider bearing.

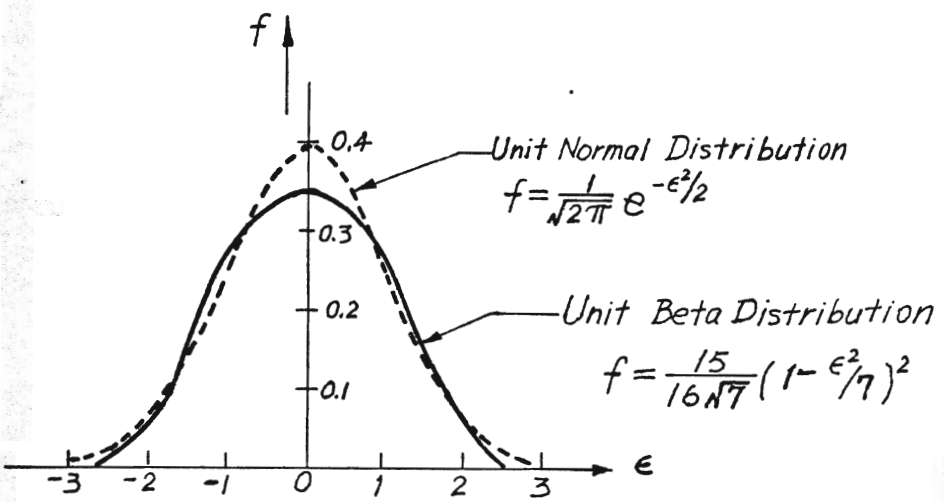

Fig. 5.4 Comparison of Beta and Gaussian distributions.

$$f(\epsilon) = \frac{15}{16c}\left(1 - \frac{\epsilon^2}{c^2}\right)^2, \text{ for } -c \leq \epsilon \leq c,$$

$$= 0, \text{ elsewhere,} \qquad \ldots\ldots\ldots\ldots\ldots\ldots\ldots\ldots \quad (5.13)$$

or in terms of the variance σ^2,

$$f(\epsilon) = \frac{15}{16(7^{1/2})\sigma}\left(1 - \frac{\epsilon^2}{7\sigma^2}\right)^2, \text{ for } -(7^{1/2})\sigma \leq \epsilon \leq (7^{1/2})\sigma,$$

$$= 0, \text{ elsewhere.} \qquad \ldots\ldots\ldots\ldots\ldots\ldots\ldots\ldots (5.14)$$

Roughness is frequently regarded as being characterized by a Gaussian distribution. Recently Williamson (34) has verified such Gaussian distributions for a wide variety of arbitrary surfaces. However, using Beta distribution as an approximation can also lead to accurate results since the analysis is not sensitive to the approximation of the distribution function. The unit Beta density function is compared with the unit Gaussian distribution in Fig. 5.4 for classification.

Now using equation (5.13) in equation (5.6) and then equation (5.4), it can be shown that

$$\left\langle \frac{dp}{dx} \right\rangle = \frac{15}{16c}\left\{\Lambda_1\left[-\frac{16c^3}{3} + 8ch^2 + 4h(c^2 - h^2)\ln\left(\frac{h+c}{h-c}\right)\right]\right.$$

$$\left. - \Lambda_2\left[12ch + 2(c^2 - 3h^2)\ln\left(\frac{h+c}{h-c}\right)\right]\right\}, \qquad \ldots\ldots\ldots\ldots\ldots (5.15)$$

$$\langle p(x) \rangle = \frac{15}{16c^5}\left\{\Lambda_1\left[\frac{-16}{3}c^3 x + \frac{8c}{m}(h^3 - h_o^3) - 4I_3 + 4c^2 I_1\right]\right.$$

$$\left. - \Lambda_2\left[\frac{6c}{m}(h^2 - h_o^2) - 6I_2 + 2c^2 I_o\right]\right\}, \qquad \ldots\ldots\ldots\ldots\ldots (5.16)$$

where h_o is the minimum value of $h(x)$, m the angle of inclination of the

shoe and

$$I_n(x) = \int_0^x h^n \ln\left(\frac{h+c}{h-c}\right) dx. \quad \text{(see 33)} \quad \ldots\ldots(5.17)$$

The total load can now be calculated from equation (5.8) as

$$\bar{W} = \frac{15}{16c^5}\left\{\Lambda_1\left[\frac{-8}{3}c^3\ell^2 + \frac{8c}{3m}\left(\frac{h_1^4 - h_0^4}{4m} - h_0^3\ell\right) - 4J_3 + 4c^2J_1\right]\right.$$

$$\left. + \Lambda_2\left[-\frac{6c}{m}\left(\frac{h_1^3 - h_0^3}{3m} - h_0^2\ell\right) + 6J_3 - 2c^2J_0\right]\right\}, \quad \ldots\ldots(5.18)$$

where $h_1 = h_0 + m\ell$ is the maximum value of h(x) and

$$J_n \equiv \int_0^\ell I_n(x)\, dx. \quad \ldots\ldots(5.19)$$

Similar calculations for the frictional forces from equations (5.9) and (5.10) yield

$$\bar{F}_1 = \frac{-15}{16c^5}\left[\frac{\Lambda_1}{3}\Psi_1 + \frac{\Lambda_2}{2}\Psi_2\right], \quad \ldots\ldots(5.20)$$

$$\bar{F}_2 = \frac{15}{16c^5}\left[\frac{2\Lambda_1}{3}\Psi_1 + \frac{\Lambda_2}{2}\Psi_2\right], \quad \ldots\ldots(5.21)$$

where $\Psi_1 = 1_4(\ell) - 2c^2I_2(\ell) + c^4I_0(\ell) + \frac{5c^3}{3m}(h_1^2 - h_0^2)$

$$- \frac{c}{2m}(h_1^4 - h_0^4), \quad \ldots\ldots(5.22)$$

and $\Psi_2 = \frac{-16}{3}c^3\ell + \frac{8c}{m}(h_1^3 - h_0^3) - 4I_3(\ell) + 4c^2I_1(\ell). \quad \ldots\ldots(5.23)$

A set of curves can be plotted from the foregoing results to tackle any

general case. For the present discussion, results are computed for a particular example to illustrate the method discussed above.

5.4 Numerical example and calculations:

Consider the example of slider mechanism as shown in Fig. 5.3 using lubricant with a viscosity of .000005 Reynolds, the velocity of sliding is 320 inches per second, the inclination of shoe is zero degree five minutes, the length of slider is 2 inches, and the roughness of the surfaces can be represented by Beta distribution with c = .0002 in. and h = .0003 in. Then by substituting $\mu = 5 \times 10^{-6}$ Reynold, U = 320 in. per second, m = tan 0°5' = .00145, ℓ = 2 in., c = .0002 in. and h = .0003 in. into equations (5.16), (5.18), 5.20) and (5.21) we get the results:

the expected unit pressure at the middle of the shoe,

$$\langle p(1) \rangle = 10{,}680 \text{ p.s.i.},$$

the expected value of the total load-carrying capacity per unit width,

$$\overline{W} = 14{,}610 \text{ lbs. per in. width},$$

the expected values of resistance force per unit width on the shoe and slider are

$$\overline{F}_1 = 5.53 \text{ lbs. and } \overline{F}_2 = 9.84 \text{ lbs.}$$

respectively.

Assuming smooth surfaces and using results of Shaw and Macks (35) the following values are obtained for the parameters:

Unit pressure at middle of the shoe, p(1) = 7,900 p.s.i.,

load carrying capacity per unit width, $\overline{W}$ = 11,250 lbs./in.,

resistance force on shoe, $\overline{F}_1$ = 6.65 lbs./in.,

resistance force on slider, $\overline{F}_2$ = 8.28 lbs./in..

The coefficients of friction, defined by $\overline{F} / \overline{W}$, are calculated as follows:

	Coefficient of friction	
	on the slider	on the shoe
Rough surfaces	.000675	.000378
Smooth surfaces	.000735	.000591

A comparison of the foregoing sets of results reveals rather interresting effects of the surface roughness. Both the load carrying capacity and the frictional forces are increased considerably when surface roughness is taken into account. However, the increase in the total load carrying capacity is more significant than that of frictional forces. This leads a lower average coefficient of friction (defined by $\bar{F} / \bar{W}$) in the case of rough surfaces than in the case of smooth surfaces.

It must be pointed out here that the analysis adopted for the problem is not just limited to an assumption of a Beta distribution. For other types of distribution there may be some difficulty in obtaining solutions in a closed form. In such an event, numerical techniques may be employed for solution. The Beta distribution when applied to such problems has certain special merits over other types of distributions. For instance, the singularities in the integrand in equation (5.6) which may arise for other types of distributions can be avoided if a Beta distribution is employed. It is felt that there are probably many instances where the surface roughness can be approximated by Beta distribution with a reasonable accuracy. This may be achieved by adjusting the powers of the density function or adjusting the maximum value of c, or both.

5.5 Summary:

The result of Spragg's test (5) shows that above the transition point the oil film thickness between two parallel bearing surfaces

increases with an increase in speed, and decreases with an increase in surface roughness. Scratch marks carefully distributed in a favorable lay is helpful in improving load carrying capacity. Salama (32) proves that the waviness with proper amplitude and pitch artificially lapped on one member of the flat thrust bearing could increase its load carrying capacity and decrease its frictional force. The solution of the slider mechanism by a stochstic random process, taking the combined effect of waviness & roughness as a Beta distribution, gives results with a reasonable accuracy. A set of curves can be plotted from these resulting equations for different values of the parameters to tackle any general problem. From the results of numerical examples one may conclude that by taking the degree of roughness into account both the load carrying capacity & frictional forces are increased. But the increase in the former is more significant with a reduction in the resulting coefficient of friction.

CHAPTER 6

BEARING CAPACITY AND FRICTIONAL RESISTANCE

6.1 Bearing area and bearing curve.

When a nominally flat surface is placed in contact with another smooth surface, kinematic principles indicate that, when no load is applied, not more than three of the highest points of the surfaces are in contact. When the load is applied, the areas of contact spread out under elastic and eventually under plastic deformations. Bowden and Tabor (6), using electrical resistance and other methods, have shown that the total area of contact is proportional to the load, thus accounting for the laws of friction. The principles holds good even for well-lapped surfaces. The initial points of contact can also be expanded by progressive lapping representing wear and the area of real contact then being that in contact with the lap. In all the cases, the area of contact is called the bearing area.

An estimate of the bearing area is often derived from a profile graph by drawing lines, such as p-q in Fig. 6.1(a), equidistant from the reference axis and measuring the sum of the metal intercepts along its length. Making assumption that the profile extends uniformly across the surface in the direction normal to the plane of the section, the proportion of the intercepts to the length of the line will indicate the proportion of true to apparent bearing area that might be expected after a certain amount of lapping. The position of the bearing line is often defined in terms of its distance below the extreme peaks expressed as a fraction of the total height, and thus involves the problem of defining this height in a satisfactory way.

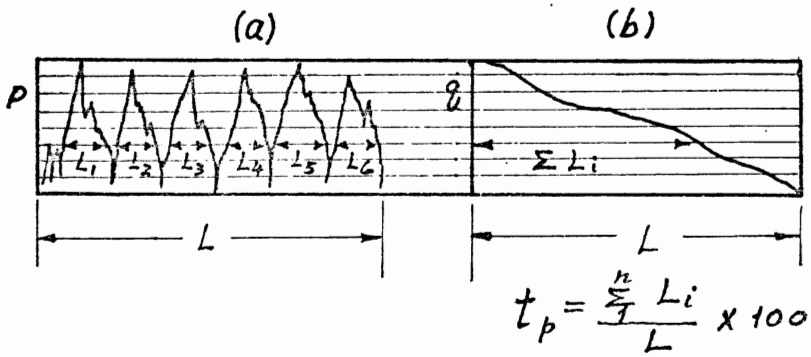

Fig. 6.1 Bearing area curve. Equation (2.6)

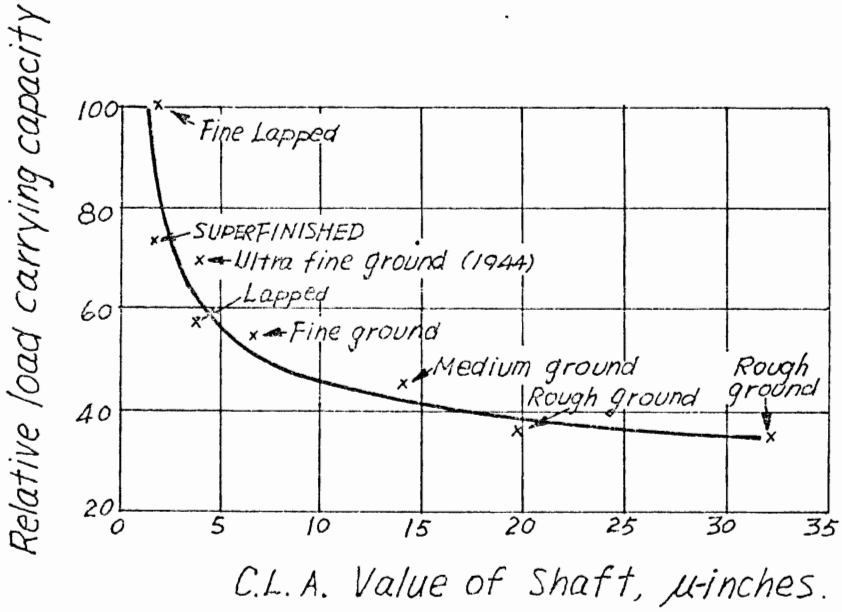

Fig. 6.2 Clay's results (4) on load carrying capacity with respect to C.L.A. values.

From the measurement of the intercepts along a number of bearing line Abbott and Firestone (5) obtained their well know "bearing area curve", as shown on Fig. 6.1(b), which gives an indication of the rate at which the wear may be expected. Ehrenreich (5) has suggested that the slope of the curve could be a useful index of performance.

The bearing area curve can also be obtained by means of the amplitude density curve plotter as described in Section 3 of Chapter 3.

6.2 Load carrying capacity:

When a hardened shaft runs in a soft bush, a fine finish at least on the surface of the shaft is required for a friction free performance. Different surface roughness has different load carrying capacity. The results of some experiments carried out by Clay (5) of Rolls Royce Co. are shown in Fig. 6.2. The plot shows the relative load carrying capacity of nitrided shafts finished in various ways, all running at 1500 r.p.m. in diamond-turned lead-bronze bushes finished to 20 micro-inches CLA with .001 diametrical clearance and D.T.D. 109 Silvertown p.4 oil lubrication.

Roughly a ten-fold improvement in the finish of the shaft resulted in a three-fold increase in the load carrying capacity as the shaft was changed from rough grinding to fine lapping. The use of oils of very low viscosity enables the machine tool spindle to run cool, but fine finishes are then required, clearance have to be reduced and alignment correspondingly improved. Special attention must be paid to the filteration of the oil and the resulting performance and long life can be rewarding (see 5).

Furey (36) studied the effect of the surface roughness and lubricant viscosity on the load carrying capacity by using one of pure sliding, but relatively high, contact stress. A fixed ball riding on a rotating

steel cylinder was employed. The mineral oils of same type (parraffinic) but varying in viscosity were evaluated in the ball-on-cylinder device. A summary of results obtained is shown in Table 6.1 as follows.

Table 6.1 Effect of surface roughness and lubricant viscosity on the load carrying capacity (36).

	Load carrying capacity W 20 (grams)	
Type of surface preparation	Sand Blasting	Machine Grinding
Surface roughness (CLA micro-in.)	94 to 106	8 to 10
Lubrication Viscosity at 77°F (cp).		
34.9	28	11
234	69	81
435	91	212

Here the load carrying capacity W20 is the load required to produce metallic contact for 20% of the time. From these results, it may be seen that increasing the viscosity by a factor of over 12 increases the load carrying capacity of the smoother machine-ground surfaces to a factor of about 20, but for the rougher sandblasted surfaces the increase is only 3 times. Alternately, for oils of low viscosity the sandblasted surfaces have 3 times the load carry capacity as compared with smooth surfaces. For higher viscosity lubricants the machine-ground surfaces exhibit twice the load carry capacity than those obtained by sand-blasting.

6.3 Surface roughness and coefficient of friction:

Surface roughness has a decided influence on the coefficient of boundary friction. Typical test results are reported by Burwell (38) for different surface roughness as measured in microinches, root mean square, on the Abbott Profilometer as shown in Table 6.2 attached.

Table 6.2 Coefficient of friction as influenced by surface roughness (38).

Surface roughness root mean square in micro-inches.	Super finish 2	Ground 7	Ground 20	Ground 50	Ground 65
Coefficient of friction for					
(i) Mineral oil	.128	.189	.360	.372	.378
(ii) Mineral oil + 2% Oleic acid	.116	.170	.249	.261	.230
(iii) Oleic acid	.099	.163	.195	.222	.238

The interesting fact is that the friction increases with roughness up to 20 microinches, after which it remains essentially a constant. The slight drop in the friction values at 65 microinches for ground surfaces in case (ii) may be due to the very fast feed that had to be used. This imparts a slight sipral texture that might have caused an erroneous reading of the roughness value by the profilometer (see 37, 38).

Miyakawa (39) reports the effect of surface roughness on boundary friction under various conditions of loads, speeds, and lubricants. From his experiments, it may be found that the direction of polishing relative to the direction of sliding greatly influences the boundary friction. For a sliding parallel to the direction of polishing, the friction is larger than sliding in the perpendicular direction to polishing. Here the average degree of roughness has very little influence upon

the friction, except in the extreme cases of very low or very high roughness values. It may be then concluded that effective lubrication takes place, when the sliding surface is perpendicular to the direction of polishing and the surface has an average degree of roughness.

6.4 Conclusions:

When two surfaces are rubbing against each other, some wear is expected to result. Bearing area curves enable rates of wear to be estimated, and can be constructed from surface traces, or can be obtained through amplitude density curve plotter.

Generally the load carrying capacity of surfaces will increase with an improvement in the surface finish, providing other conditions remain the same. The increase of lubricant viscosity has an advantageous effect on the load carrying capacity of a smoother surface than that of a rougher surface.

The boundary friction is markedly affected by the direction of sliding rather than the degree of surface roughness. However, the roughness provides the effective lubricating action as a result of the interruption of contact by the roughness of the surfaces. A desirable lubrication effect takes place when the sliding surface is perpendicular to the direction of polishing and the surface has an average degree of roughness.

CHAPTER 7

SURFACE ROUGHNESS AND CORROSION PROPERTIES

7.1 Introduction:

By definition corrosion is the destruction of a metal by chemical or electro-chemical reaction with its environment. The majority of corrosion is caused by liquid and gaseous agents. This involves the loss of electrons from the metal atoms - known as 'oxidation', and gain of electrons by the atom in the reaction agents - known as 'reduction'.

7.2 Stress corrosion:

The distortion of metal under stress is very much like the dislocation of grain boundaries in the case of corrosion. For any local disorder, there is an increase in local energy and the distorted material becomes increasingly anodic. The result is a localized decrease in resistance to corrosion. In the stress - corrosion cracking, where the grain boundaries become sufficiently anodic, the average stress level is almost near the yield point. The corrosion attack starts at the grain boundaries that are situated in a plane perpendicular to the plane of the tensile stress. As the stress corrosion penetrates, notches will start forming between the grains, and the local stress on the grain boundaries increases. Since the stress on a boundary depends on the loading and the bearing area, which in turn is dependent on the roughness texture, it may be concluded that surface roughness affects stress - corrosion directly.

Rough surfaces generally possess what is called 'stress raisers', minute scratches on the surface having the local stress concentrating

affect. The flaws in the material can also add to this affect causing some transcrystalline corrosion. All these factors cause a rapidly propagating corrosion and the grains are gradually pulled apart by the resulting tensile stress. The end result is a fracture with little or no plastic deformation of the metal.

Residual stresses are particularly important in this type of corrosion propagation. For example ground surfaces usually leave some residual stress in the underlay. Lapping or honing operations generally produce a finer texture with a lower tendency to corrosion because they reduce the residual stresses. Shot - peening results in a higher roughness, but it introduce some compressive residual stresses which actually counteracts propagation of stress corrosion (see 42, 43).

7.3 Corrosion - fatigue:

The influence of the atmosphere on fatigue life is considerable. In corrosive atmosphere, repeated cycling and corrosion seem to interact and the damage is greater than the simple summing of the two indepently. This interaction of corrosion and fatigue is called corrosion fatigue.

The progress of corrosion depends on time, while failure due to fatigue depends on the number of cycles of repeated stress. Hence the corrosion - fatigue will be sensitive to changes in the rate of stress cycling. The experimental results of Lessells (43) indicates that in corrosive atmosphere a fatigue limit does not exist. All factors that affect fatigue will also contribute to corrosion - fatigue.

Rough surfaces tend to have more stress raisers and hence are more likelihood of initiating fatigue cracks. The formation of fatigue cracks at corrosion pits intensifies the stress at the tip of the crack, thus increasing the corrosion rate further. Corroded particles tend to fill

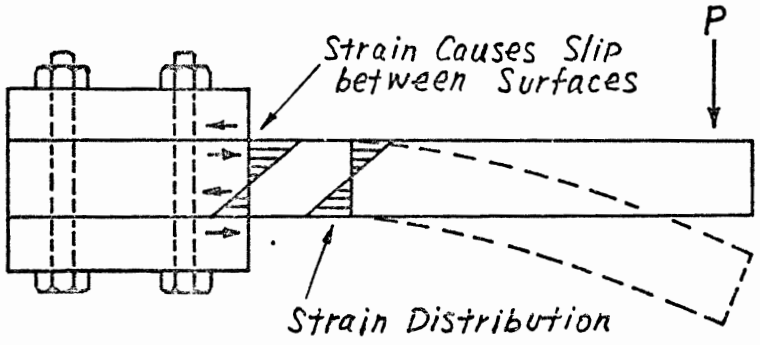

Fig. 7.1 An example of Fretting Corrosion.

the fatigue cracks, preventing the formation of protective films and exerting a wedging action on the sides of the crack, thus propagating the crack further (see 43).

7.4 Fretting - corrosion:

Fretting - corrosion occurs frequently in these components that are intended to be clamped together so tightly as to prevent any relative movement. The elasticity of the components makes a perfect clamping difficult if not actually impractical in many instances.

As an example consider a bar that is clamped between two blocks as shown in Fig. 7.1. When the cantilever bends downward due to the applied loads, the highest tensile stress occurs on the uppermost fibres of the bar which is adjacent to the clamping block. This stress is transmitted to the material between the blocks and through friction to the block itself. Under ordinary conditions, the friction is insufficient to prevent slipping at this interface and hence fretting will result. A similar situation occurs in a ball bearing race that is pressed onto a shaft. Other examples are shrunk - fit collars, bolted and riveted joints subject to vibrations, and splined shafts. The fretting can be reduced by increasing the friction between the interfaces that is by increasing the roughness of the surfaces in contact.

Obviously, if slipping can be completely prevented, fretting corrosion will be eliminated. One remedy is to increase the tightening pressure and also increase the friction by roughening the contact surfaces. Another possibility is to counteract the tensile stresses by introducing compressive residual stresses on the surface where fretting due to slipping is expected to occur (see 42).

7.5 Conclusion:

Increased surface finish increases the resistance to stress-corrosion. Residual stress plays an important role in stress - corrosion effect. Tensile residual stresses accelerate corrosion propagation whereas compressive stresses counteract corrosion. Such effects can be obtained by a proper choice of surface finishing operation. Lapping or honing reduces the residual stresses on the surface and hence in these cases there is less tendency to corrosion. Shot peening produces compressive residual stress and therefore beneficial in the prevention of stress - corrosion.

Rougher surfaces tend to have more stress raisers and hence chances are great for an initiation of fatigue cracks. All the factors that affect fatigue strength of specimen also affect corrosion-fatigue.

Increased surface roughness increases the frictional force between the contacting surfaces thus reducing fretting-corrosion. Introduction of compressive residual stresses on the surface also prevents slipping and hence fretting - corrosion.

CHAPTER 8

CONCLUDING REMARKS

Since the performance of a manufactured product is always affected by the texture of its surfaces both the design and the manufacturing engineers have become, in the recent years, greatly interested in the exact specification and control of the integrity of the surface involved as well as in the establishment of some correlation with the resulting mechanical properties.

In this technical report the theories of surface texture specifications and the techniques for their measurement are critically discussed. Analytical approaches and experimental results of previous investigators on the effect of surface roughness on its mechanical properties are also studied in detail.

Most of the existing specifications are based on the peak-to-valley measurement as an indication of the roughness. Due to its simplicity in assessment and convenience for adoption in instrumentation, the CLA (center line average) measure is, up to now, the most widely accepted standard for specifying and controlling the surface qualities. Since statistical descriptions are consistent with the character of the manufactured surfaces, a specification arising out of such methods will provide a rigorous procedure to give exact nature of the texture of any profile. Experimental results obtained by the author and reported in this dissertation verifies this point.

Aside from the effect of surface irregularities, the residual stresses on the surface have a deciding influence on the resulting fatigue strength. Surfaces produced by different processes may have the same roughness values, but different fatigue strengths. Those having compressive

residual stresses and higher surface hardness usually have higher fatigue strengths. It is concluded that both carburizing and nitriding can increase the fatigue strengths considerably. For increased hardness of the surface, an increase in the quality of surface finish improves the fatigue strength and life of the specimen.

As far as the retainment of lubrication is concerned, both the primary and secondary textures of the surface irregularities are essential. The result of Spragg's test shows that above the transition point the oil film thickness between two parallel bearing surfaces increases with an increase in speed, and decreases with an increase in surface roughness. It is also seen that waviness with proper amplitude and pitch can increase the load carrying capacity of a flat thrust bearing. Using a method based on a probabilistic approach the load carrying capacity and frictional forces can be computed for a slider mechanism if the conditions of lubrication are known.

Bearing area curve provides a useful means for the estimation of wear resistance. It can be obtained either from the surface profile trace or directly through the amplitude density curve plotter. An increase in the quality of the surface finish generally increases the load carrying capacity. Increased viscosity of lubricant yields higher bearing load capacity on a smooth surface than on a rough surface. When two surfaces with average roughness are rubbing together in such a way that the direction of sliding is perpendicular to the direction of polishing of the surface, a higher load carrying capacity and less frictional force on the interface can be expected. All factors that improve fatigue strength, reduce friction, and increase bearing capacity are benificial for corrosion resistance.

It is evident from this presentation that a theoretical definition of a surface profile and its influence on the performance of the associated component is an extremely complex problem. All the existing theories and subsequent experimental findings have succeeded only in establishing relations that are empirical with little mathematical foundations. In the recent years attempts have been made to solve this problem employing the mathematical theory of stochastic processes. Though the available information is scarce and mostly incomplete, it may be recognized that investigations directed along these lines have the prospects of success and achieving satisfactory results useful for design.

LIST OF REFERENCES

(1) Reason R.E., Hopkins M.R. & Garrod R.I., Report on the measurement of surface finish by stylus methods, May 1966, Rank Taylor Hobson Co. England.

(2) Talysurf No. 4, Operator's instruction book, Rank Precision Industries Ltd, Metrology Division, Leicester House, Lee Circle, Leister, England.

(3) Reason R.E., Concepts of accuracy in surface profile measurement, Proceedings of International Conference on Manufacturing Technology University of Michigan, Ann Arbor, Michigan, September, 1967, pp. 1285 - 1301

(4) F.P. Bowden, M.A. Stone, G.K. Tudor, Proc. Roy. Suc. A. Vol. 188, pp. 329 - 349.

(5) H. Wright Baker, Modern Workshop Technology, 1967, Macmillan & Co. Ltd, London, pp. 413 - 485.

(6) Bowden F.P. & Tabor D., The friction and lubrication of solids. Clarendon Press, Oxford, 1954.

(7) L.C. Martin & B.K. Johnson, Practical microscopy.

(8) D.J. Whitehouse, R.E. Reason, The equation of the mean line of surface texture found by an electric filter. Rank Taylor Hobson Co. England.

(9) A. Wirtz, Die Kennzeichnung der Rauheit geschliffener Oberflächen, Technische Rundschau, No. 47, Bern, 1962. (Report from the machine tool Lab. of the ETH.)

(10) Bickle, E. Some Fundmental problems in the measurement of surface roughness, International Research in Production Engineering, Proceedings of the International Production Engineering Research Conference, Pittsburgh, 1963, ASME (1963) pp. 667 - 674.

(11) M. Pesante, Determination fo Surface roughness typology by means of Amplitude density curves, CIRP Annalen 12 (1963/64), No. 2, pp. 61 - 68.

(12) J. Wallach, Surface Topography description and measurement, Surface Mechanics, The ASME Winter Annual Meeting, November 16 - 21, 1969, Los Angeles, California.

(13) M.F. Spott, Design of machine elements, 1961, Prentice Hall, New York, pp. 511.

(14) H. Von Weingraber, The geometrical state of the surface of a solid, International Conference on Manufacturing Technology, Sept. 1967, pp. 1271 - 1277.

(15) W.E. Littmann, Control of Residual stress in metal surfaces. Proceedings of the International Conference on Manufacturing Technology, University of Michigan, Ann Arbor, Michigan, September, 1967, pp. 1303 - 1317.

(16) R. Von Hasselt, Resume and critique of papers on surface quality, Proceeding of the International Conference on Manufacturing Technology, University of Michigan, Ann Arbor, Michigan, September 1967, pp. 1265 - 1284.

(17) Moore, H.F. and J.B. Kommers, An Investigation of the fatigue of metals, Univ. Ill. Eng. Exp. Sta. Bull. 124, 1921.

(18) Thomas, W.N., Effect of scratches and of various workshop finishes upon the Fatigue Strength of Steel, Engineering, Vol. 116, 1923, pp. 449 - 454, 483 - 485.

(19) Siebel, E. and M. Gaier, Influence of surface roughness on the fatigue strength of steels and non-ferrous alloys, Metal Progr. Vol. 73, January, 1958, pp. 174.

(20) Caswell, J.S., Effect of surface finish on fatigue limit of Mild steel, Product. Eng. Vol. 18, March, 1947, pp. 152.

(21) Fluck, P.G., The influence of surface roughness on the fatigue life and scatter of test results of two steels, ASTM Proc. Vol. 51, 1951 pp. 584 - 592.

(22) Noll, G.C. and C. Lipson, Allowable Working Stresses, Proc. Soc. Exp. Stress Analysis, Vol. III, No. II, 1946, pp. 89 - 101.

(23) Noll, G.C., and M.A. Erickson, Allowable stresses for steel members of finite life, Proc. Soc. Exp. Stress Analysis, Vol. V, No. II, 1949, pp. 132 - 143.

(24) M.P. Rubert, Contradiction in surface roughness measurement, Advances in Machine Tool Design and Research, 1966, Symposium Publications Division, Pergamon Press.

(25) Cina, B., Effect of Surface Finish on Fatigue, Metallurgia, Vol. 55, January, 1957, pp. 11 - 19.

(26) Sinclair, G.M., H.T. Carten, and T.J. DOlan, Effect of surface finish on the fatigue strength of titanium alloys RC 130B and Ti 140A, ASME Trans. Vol. 79, No. 1, January, 1957, pp. 89 - 96.

(27) Austin, C.R., Effect of surface decarburization on the fatigue properties of steel, Metals & Alloys, Vol. II, September, 1931, pp. 117 - 119.

(28) Horger, C.J., Fatigue strength of members as influenced by surface conditions, Product Eng., Vol. 12, January, 1941, pp. 22 - 24.

(29) Wiegand, H., Effect of surface treatment on fatigue strength, MAP Translation 1772, BMW Flugmotorenbau, Berlin, 1940.

(30) Zimmerli, F.P., Shot blasting and its effect on fatigue life, Surface Treatment of Metals, by ASM, 1944, pp. 261 - 278.

(31) Bowden, F.P., & Tabor, D., Proc. Roy. Soc. Vol. 169A, 1939.

(32) Bowden, F.P., & Moore, A.J.W., Nature, Vol. 155, April, 1945, pp. 451 - 452.

(33) Bisson, E.E. and Anderson, W.J., Advanced Bearing Technology, NASA, Washington, D.C., 1964.

(34) Williamson, J.B.P. (Private communication).

(35) Shaw, M.C. & Macks, E.F., Analysis of Lubrication of Bearings, McGraw Hill, 1949, New York.

(36) M.J. Furey, Surface roughness effects on metallic contact and friction, ASLE Transaction 6, 1963, pp. 49 - 59.

(37) Dudley D. Fuller, Theory and practice of lubrication for engineer, John Wiley & Sons, 1960, New York, pp. 355.

(38) Burwell J.T., The role of surface chemistry and profile in boundary lubrication, SAE Journal Vol. 50, 1942, pp. 450.

(39) Yukio Miyakawa, Influence of surface roughness on boundary friction, Presented on 20th ASLE anual meeting in Detroit, May, 1965.

(40) J.G. Tweeddale, Metallurgical principles for engineers, Iliffe Books Ltd, London, pp. 379.

(41) Hughes and Gaylord, Basic equations of engineering science, Schaum Publishing Co. New York, pp. 48.

(42) Cedric W. Richards, Engineering material science, Wodsworth Publishing company, San Francisco, pp. 494 - 498.

(43) Frank A. McClintock & Ali S. Argon, Mechanical behavior of materials, Addison Wesley Ltd, Don Mills, Ontario, pp. 606.

(44) S.T. Tzeng and Edward Saibel, Surface roughness effect on Slider bearing lubrication, ASLE Transaction 10, 1967, pp. 334 - 338.

LEGEND FOR FIGURES

Fig. 2.1 General case of scratch texture due to tool abrasion.

Fig. 2.2 Peak to valley measure.

Fig. 2.3 The Swedish method.

Fig. 2.4 Mean line measure (CLA).

Fig. 2.5 Crest line measures.

Fig. 2.6 Bearing ratio curve.

Fig. 2.7 Principal parts of stylus device.

Fig. 2.8 Rounded skid and swiveling shoe adopted in stylus devices.

Fig. 2.9 Effect of wave form on skid movement.

Fig. 2.10 Electrical Magnifying, device with circuits:
(a) for carrier modulating instrument,
(b) for current generating instrument,
(c) for potential generating instrument.

Fig. 2.11 Operative effect (transmission characteristic) of electric wave-filter.

Fig. 2.12 Line diagram of R-C networks of wave-filter.

Fig. 2.13 Transmission curves of standard R-C wave-filter.

Fig. 2.14 Block diagram of Talysurf No. 4 instrument.

Fig. 2.15 (a) Roughness profile in medium turning, X2000V, X100H, CLA = 5.3μm. 0.1 in. cut-off.

Fig. 2.15 (b) Roughness profile in semi-finish turning, X2000V, X100H, CLA = 3.5μm. 0.1 in. cut-off.

Fig. 2.15 (c) Roughness profile in finish turning, X2000V, X100H, CLA = 2.5μm. 0.1 in. cut-off.

Fig. 2.15 (d) Roughness profile in milling, X2000V, X100H, CLA = 5.7μm. 0.1 in. cut-off.

Fig. 2.15 (e) Roughness profile in grinding, X2000V, X100H, CLA = 1.7μm. 0.1 in. cut-off.